

**LASER INDUCED BREAKDOWN SPECTROSCOPY (LIBS) AND
TIME-RESOLVED STUDIES OF COPPER PLASMA EXCITED BY
NANOSECOND AND FEMTOSECOND LASER PULSES**

*A project report submitted to the Cochin University of Science and Technology
for the award of five year integrated Masters of Science Degree in Photonics
(2007-2012)*



**Submitted by
Anusha Keloth
X Semester
5 Year Integrated MSc in Photonics
Centre of Excellence in Lasers and Optoelectronic Sciences (CELOS)
Cochin University of Science and Technology (CUSAT)**

**Under the guidance of:
Dr. Reji Philip
Associate Professor
Raman Research Institute
Bangalore**

DECLARATION

I hereby declare that the project report entitled "**Laser induced breakdown spectroscopy (LIBS) and time-resolved studies of copper plasma excited by nanosecond and femtosecond laser pulses**" comprises of my original work carried out under the guidance of Dr.Reji Philip, Associate Professor, Raman Research Institute, Bangalore.

Anusha Keloth

ACKNOWLEDGMENT

It has been a wonderful experience for me to be a part of the Ultrafast and nonlinear optics group at Raman Research Institute, Bangalore. With immense pleasure, I express my proud gratitude and indebtedness to my supervising guide Dr. Reji Philip, Associate Professor Raman Research Institute, Bangalore for giving me an opportunity to do my project with his group and for his valuable suggestions and help throughout the period of my work.

I am grateful to the Director Prof.P Radhakrishnan, ISP, CUSAT for his support and encouragement throughout my studies.

I also express my sincere gratitude to the Project assistant Anoop for his guidance and constant support in completing my project. I would like to thank Dr. Priya Rose T, Post Doctoral Fellow, RRI for her motivation and support. I would also like to thank Mr. Jinto Thomas, Scientist, Institute for Plasma Research, Gandhinagar for his valuable suggestions.

I also thank other lab members Shafi and Maduri, for their support and help. I am thankful to all my teachers and friends for their encouragement and cooperation for completing the project.

It is a great pleasure for me to thank my parents and my brother, without their valuable support, this thesis would not have been possible.

Above all, I thank GOD, for leading me kindly along the twists and turns of life and for giving me strength to carry out this work well.

Anusha Keloth

To My Parents & Brother

Preface

In the discipline of spectroscopy, invention of lasers was a technological revolution. The interaction of laser light with materials, and the properties of the plasma produced by focusing high peak power laser radiation onto a solid target, is an area of ongoing development in basic science, engineering, and materials processing. In laser induced breakdown spectroscopy (LIBS), a pulsed laser source is employed to excite and vaporize a target, which results in the formation of a plasma. Useful information about the elemental composition of the target material can be obtained by analyzing the spectral emission of the plasma plume. LIBS is an excellent technique for quick, real-time elemental analysis. The work presented in this thesis is an investigation of the emission and temporal evolution of spectral lines in a laser-induced copper plasma, excited by laser pulses of 100 femtosecond and 7nanosecond durations respectively.

The thesis is laid out in six chapters. Chapter 1 gives an introduction to plasma physics and laser-induced plasmas. Basic plasma parameters are discussed here. Chapter 2 is a brief review of laser induced breakdown spectroscopy, in which the advantages and applications of this powerful analytical technique are discussed. Chapter 3 discusses the instrumentation part, giving details of the devices and apparatus used for the LIBS and temporal evolution studies reported in this work. Chapter 4 presents the LIBS study of femtosecond and nanosecond laser-induced copper plasma. In this chapter, the effect of ambient pressure and laser energy on the emission spectra is studied for both femtosecond and nanosecond excitation regimes. The plasma temperature and number density are calculated from standard equations. Chapter 5 describes the time resolved spectroscopic study of femtosecond laser-induced copper plasma. Temporal evolution of the plasma plume recorded using an Intensified CCD (ICCD) camera is discussed. The lifetimes of neutral copper atom measured at different background pressures also is presented. Chapter 6 gives the conclusion and future outlook of the work done.

CONTENTS

Chapter 1	Introduction to Laser Induced Plasma	Page No
	1.1 Introduction	1
	1.2 Plasma Parameters	1
	1.3 Laser Induced Plasma	4
	1.4 Laser Ablation of Solid Target	6
	1.5 Theory	7
Chapter 2	Laser Induced Breakdown Spectroscopy (LIBS)	
	2.1 Introduction	9
	2.2 Advantages of Laser Induced Breakdown Spectroscopy	11
	2.3 Applications of Laser Induced Breakdown Spectroscopy	13
Chapter 3	Instrumentation for Laser Induced Breakdown Spectroscopy and Time Evolution Studies	
	3.1 Introduction	15
	3.2 Laser System	16
	3.3 Sample Chamber	19
	3.4 Imaging and Detection	21
Chapter 4	Laser Induced Breakdown Spectroscopy Studies of Copper Using Nanosecond and Femtosecond Laser Pulses	
	4.1 Introduction	25
	4.2 Experimental Setup	25
	4.3 Results and Discussions	
	a) Emission Studies	27

	b) Determination of electron temperature and number density of plasma	30
	c) Effect of laser energy	33
Chapter 5	Time-Resolved Spectroscopic Study of Femtosecond Laser Induced Copper Plasma	
	5.1 Introduction	35
	5.2 Experimental Setup	35
	5.3 Results and Discussions	
	a) Imaging Results and analysis	37
	b) Characteristics of lifetimes with pressure change	39
Chapter 6	Conclusions and Future Outlook	42
References		44

CHAPTER 1

INTRODUCTION TO LASER INDUCED PLASMA

1.1 Introduction

Plasma is often called the "Fourth State of Matter". Plasma is a distinct state of matter containing a significant number of electrically charged particles, a number sufficient to affect its electrical properties and behavior. In addition to being important in many aspects of our daily lives, plasmas are estimated to constitute more than 99 percent of the visible universe. Earthbound plasmas include lightning, fluorescent lighting, arc welders, and computer displays. In an ordinary gas each atom contains an equal number of positive and negative charges; the positive charges in the nucleus are surrounded by an equal number of negatively charged electrons, and each atom is electrically "neutral." A gas becomes plasma when the addition of heat or other energy causes a significant number of atoms to release some or all of their electrons. The remaining parts of those atoms are left with a positive charge, and the detached negative electrons are free to move about. Those atoms and the resulting electrically charged gas are said to be "ionized." When enough atoms are ionized to significantly affect the electrical characteristics of the gas, it is plasma.

In many cases interactions between the charged particles and the neutral particles are important in determining the behavior and usefulness of the plasma. The type of atoms in a plasma, the ratio of ionized to neutral particles and the particle energies all result in a broad spectrum of plasma types, characteristics and behaviors. These unique behaviors cause plasmas to be useful in a large and growing number of applications important to our lives and to the world around us.

1.2 Plasma Parameters

An ionized gas is in the plasma state if the charged particle interactions are predominantly collective. In a plasma the interactions are collective because many charged particles interact simultaneously, but weakly, through their long-range electromagnetic fields in particular their Coulomb electric fields.

The plasma frequencies the most fundamental time-scale in plasma physics. Plasma frequency is given by

$$\omega_p^2 = ne^2/\epsilon_0 m \quad \dots\dots\dots (1.1)$$

There is different plasma frequency for each species. However, the relatively fast electron frequency is the most important. It is seen that ω_p corresponds to the typical electrostatic oscillation frequency of a given species in response to a small charge separation. Plasma oscillations will only be observed if the plasma system is studied over time periods τ longer than the plasma period $\tau_p=1/\omega_p$, and if external actions change the system at a rate no faster than ω_p . Observations over length-scales L shorter than the distance $v_t\tau_p$ traveled by a typical plasma particle during a plasma period will also not detect plasma behavior. In this case, particles will exit the system before completing a plasma oscillation. This distance, which is the spatial equivalent to τ_p , is called the Debyelength, and takes the form.

$$\lambda_D = (T/m)^{1/2} \omega_p^{-1} \quad \dots\dots\dots (1.2)$$

or

$$\lambda_D = \epsilon_0 T / ne^2 \quad \dots\dots\dots (1.3)$$

where Debye length is independent of mass, and therefore generally comparable for different species. Clearly, our idealized system can only usefully be considered to be a plasma provided that

$$\lambda_D / L \ll 1 \quad \dots\dots\dots (1.4)$$

and

$$\tau_p / \tau \ll 1 \quad \dots\dots\dots (1.5)$$

Here, τ and L represent the typical time-scale and length-scale of the process under investigation. Plasmas generally do not contain strong electric fields in their rest frames. The shielding of an external electric field from the interior of a plasma can be viewed as a result of high plasma conductivity: i.e., plasma current generally flows freely enough to short out interior electric fields. However, it is more useful to consider the shielding as a dielectric phenomenon: i.e., it is the polarization of the plasma medium, and the associated redistribution of space charge, which prevents penetration by an external electric field. The length-scale associated with such shielding is the Debye length.

Let us define the plasma parameter

$$\Lambda = 4\pi n \lambda_D^3 \quad \dots\dots\dots (1.6)$$

This dimensionless parameter is obviously equal to the typical number of particles contained in a Debye sphere

$$\Lambda = \frac{\lambda_D}{r_c} = \frac{1}{\sqrt{4\pi}} \left(\frac{r_d}{r_c}\right)^{3/2} = \frac{4\pi\epsilon_0^{3/2} T^{3/2}}{e^3 n^{1/2}} \dots\dots\dots (1.7)$$

where average distance between particles,
 $r_d = n^{-1/3} \dots\dots\dots (1.8)$

and the distance of closest approach,
 $r_c = e^2 / 4\pi \epsilon_0 T \dots\dots\dots (1.9)$

The fundamental plasma parameter, the number of charged particles in a Debye cube, depends on the plasma temperature and charged-particle density, i.e.

$$n\lambda_D^3 \propto \frac{T^{3/2}}{n^{1/2}} \dots\dots\dots (1.10)$$

It can be seen that the case $\Lambda \ll 1$, in which the Debye sphere is sparsely populated, corresponds to a strongly coupled plasma. Likewise, the case $\Lambda \gg 1$, in which the Debye sphere is densely populated, corresponds to a weakly coupled plasma. It can also be appreciated, from the equation for plasma parameter that strongly coupled plasmas tend to be cold and dense, whereas weakly coupled plasmas are diffuse and hot. Examples of strongly coupled plasmas include solid density laser ablation plasmas, the very “cold” (*i.e.*, with kinetic temperatures similar to the ionization energy) plasmas found in “high pressure” arc discharges, and the plasmas which constitute the atmospheres of collapsed objects such as white dwarfs and neutronstars.

The characteristic collective plasma behavior is only observed on time-scales longer than the plasma period and on length-scales larger than the Debye length. Although ω_p , λ_D , and Λ are the three most fundamental plasma parameters, there are a number of other parameters.

The three criteria for existence of the plasma state,

1. $n\lambda_D^3 \gg 1$. The number of charged particles within a Debye cube (or sphere) must be large so that collective interactions dominate at the mean interparticle separation distance, the energy density embodied in the polarization electric field around a given charged particle is small compared to a typical particle's kinetic energy and the thermal noise level is small

2. $L \gg \lambda_D$. The spatial extent of a collection of charged particles must be large compared to the collective interaction scale length for plasmas, the Debye length λ_D , so that the collective interactions are dominated by bulk plasma rather than boundary effects and inertial effects are determined locally.
3. $\omega_p \gg \nu_{en}$. The collective inertial response frequency in a plasma, the electron plasma frequency ω_p , must be large compared to the electron neutral collision frequency ν_{en} , so that the fundamental inertial responses, the electrostatic electron plasma oscillations and the plasma oscillation effects on electromagnetic waves, are not damped by dissipative neutral particle collision effects.

These criteria for the existence of the plasma state are applicable to magnetized plasmas as well. Among the three criteria for existence of the plasma state, the first one, the requirement that there are many charged particles in a Debye cube, is the necessary condition and the most critical. After this fundamental criterion is satisfied, the second and third criteria are just checks (sufficient conditions) that the behavior of the medium will be dominated by collective plasma phenomenon the basic plasma length and time scales.

1.3 Laser Induced Plasma

The development of high powered lasers in the 1960's opened up the field of laser plasma physics. Laser plasma can be formed on any type of a sample: solid, liquid, gas and aerosol. When a high power pulsed laser sent onto the sample, the sample absorbs the energy from the laser; heated up, melts and evaporates. Due to the high peak powers of the laser, temperatures may reach up to 20,000K. At that moment; the sample atomizes, ionizes and forms the plasma. The electric field associated with incident optical pulse accelerates the free electrons, which act to thermalise the electron energy distribution. As the electron energies grow, collisions produce ionization, other electrons, more energy absorption, and an avalanche occurs. In the photon picture, absorption occurs because of inverse bremsstrahlung. The breakdown threshold is usually specified as the minimum irradiance needed to generate visible plasma. Plasma is a luminous cloud that has time dependent characteristics. After the laser pulse is off, cooling process starts through the expansion of the plasma with a shockwave in front. During the plasma cooling, radiative emission of the light at characteristic wavelength of the sample is observed while excited atoms and ions relax back to the ground state. This atomic emission is monitored by a time resolved, gated detector.

The plasma evolves through several transient phases, between its initiation and decay as it grows and interacts with the surroundings. The three models for propagation and expansion are the laser-supported combustion (LSC), laser-supported detonation (LSD), and laser-supported radiation (LSR) waves. They differ in their energy transfer properties of the plasma to the ambient atmosphere. Plasma emits useful emission signals throughout the expansion phase. It cools and decays as its constituents give up their energies in a variety of ways. The ions and electrons recombine to form neutrals, and some of those recombine to form molecules. Energy escapes through radiation and conduction

Laser plasmas tend to have extreme properties (e.g., densities characteristic of solids) not found in more conventional plasmas. A major application of laser plasma physics is the approach to fusion energy known as inertial confinement fusion. In this approach, tightly focused laser beams are used to implode a small solid target until the densities and temperatures characteristic of nuclear fusion i.e., the centre of a hydrogen bomb are achieved. Another interesting application of laser plasma physics is the use of the extremely strong electric fields generated when a high intensity laser pulse passes through plasma to accelerate particles. High-energy physicists hope to use plasma acceleration techniques to dramatically reduce the size and cost of particle accelerators.

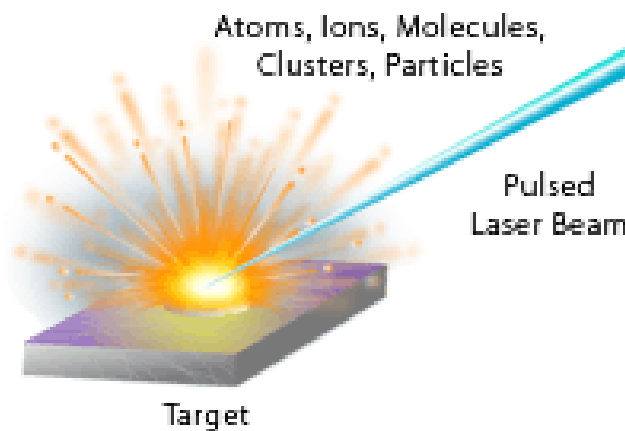


Figure 1.1: Laser induced Plasma

When laser was focused on to a metallic surface another striking effect involves production of luminous cloud of vaporized material blasted from a metallic surface and accompanied by a shower of sparks. These laser effects have found many technological applications in the field of metal working, plasma production and semiconductors. When a pulsed laser beam of high intensity is focused on to a material, it generates plasma from the material. This phenomenon of Laser induced plasma has proved to be a powerful surface analytical technique, capable of performing trace element measurements in any kind of solid material as well as in liquids, Pulsed laser deposition (PLD) and chemical trace analysis. Laser induced plasma strongly depend on incident laser Intensity (Pulse duration, laser

wavelength, irradiation spot size, focal length of the lens laser energy), ambient gas composition and ambient pressure. In recent years there has been a notable interest both in increased understanding of laser induced plasma and their applications.

1.4 Laser Ablation of Solid Target

The laser ablation process can be classified into three regimes: evaporation of the target material, interaction of the evaporated cloud with incident laser beam resulting in cloud heating and plasma formation, and expansion and rapid cooling of the plasma. Breakdown on surfaces and ablation are complex phenomena. .

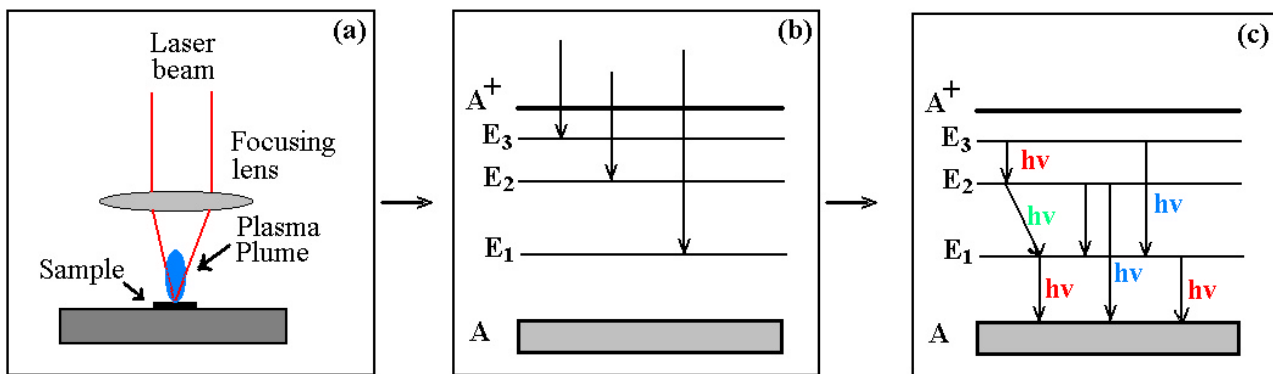


Figure 1.2: Timing of a LIPS process: (a) plasma ignition, (b) broadband emission due to Bremsstrahlung and free-bound transitions, (c) line emission due to bound- bound transitions.(ref : 24)

In the first domain, the laser heats and evaporates a small amount of the sample. The first seed electrons are created, either due to multi-photon ionization or thermal emission of the surface. Multi-photon ionization is described by the reaction



These electrons absorb further photons from the same laser pulse and transfer their energy to the atoms in the plume by collisions. Further ions are thus produced, while a shock wave is observed due to the fast heating of the gas reaching temperatures of several thousand degrees. . The energy of a single photon from lasers used to generate the spark is usually much less than the energy needed to ionize an atom. However, because of high power density (MW/cm²) and large photon flux (photons/cm²) of the focused laser pulses, there is a high probability that ionization will occur by the absorption of many laser photons during the laser pulse.

Time domain (b) is characterized by a broadband emission originating from the Bremsstrahlung of the free electrons and electron-ion recombination and it has duration of a few hundred nanoseconds. Weak lines show up on the strong continuum and they are mostly identified as ionic lines of the plume constituents. Finally time domain (c) is characterized by an emission spectrum; where narrow atomic lines dominate corresponding to the elements present in the plume and line strength is proportional to the atomic concentration. This time regime lasts for several microseconds and it is exactly the regime that is relevant for elemental analysis.

1.5 Theory

A) Rate equation for optical breakdown

The strong electromagnetic radiation fields interacting with the electrons in a condensed medium with a bandgap larger than the photon energy can lead to the generation of quasi-free electrons in the conduction band through nonlinear processes such as multiphoton ionization or the tunnel effect. These free charges can subsequently gain sufficient kinetic energy from the electric field by inverse bremsstrahlung absorption to produce more free carriers through impact ionization. The rapid ionization of the medium leads to plasma formation and to a drastic increase of the absorption coefficient, which in turn gives rise to a rapid energy transfer from the radiation field to the medium. This process is called optical breakdown or laser induced breakdown when the free electron density exceeds a critical value of 10^{18} to 10^{20} cm^{-3} . At this value, the plasma is dense enough to absorb a significant fraction of the laser light.

The break down threshold can be calculated by using the rate equation given by

$$\frac{d\rho}{dt} = \left(\frac{d\rho}{dt}\right)_{mp} + \eta_{casc} \rho - g\rho - \eta_{rec} \rho^2 \quad \dots\dots\dots (1.12)$$

where ρ is the free electron density, η_{cas} is Cascade ionization rate, η_{rec} is the recombination rate and g is the Diffusion rate.

The first term describe electron generation through multiphoton absorption $\left(\frac{d\rho}{dt}\right)_{mp}$ which acts both as a source for the cascade process and as a contributor to plasma growth and second term describes growth of electron plasma by cascade (avalanche) ionization ($\eta_{casc} \rho$). The remaining terms $-g\rho$ and $-\eta_{rec} \rho^2$ accounts for the diffusion of electrons out of the focal volume and for recombination losses respectively.

B) Multiphoton Ionization

To ionize an atom or molecule with an ionization energy ΔE , $k = \lceil \Delta E / (h\omega) \rceil$, photons are required. That is it is assumed that in order the light absorption can supply the atoms the ionization energy, many photons are absorbed simultaneously, as the ionization potentials are of the order of magnitude 10 times larger than laser quanta $h\nu$. Thus, the multiphoton ionization rate will be proportional to I^k where I is the laser light irradiance.

C) Cascade Ionization

Once quasi-free electrons are generated in the conduction band, they gain energy from the electric field through inverse bremsstrahlung absorption. Conservation of momentum requires that the absorption of photons from the laser pulse takes place during collisions of the free electrons with surrounding molecules. If each electron whose kinetic energy exceeds the ionization energy shortly produces another quasi-free electron, the cascade ionization rate per electron is given by the equation

$$\eta_{\text{casc}} = \frac{1}{\omega^2 \tau^2 + 1} \left[\frac{e^2 \tau}{4\pi \epsilon_0 m \Delta E} I - \frac{m \omega^2 \tau}{M} \right] \dots\dots\dots (1.13)$$

where ω is the Laser frequency τ is the time between electron-heavy particle collisions, n is the refractive index, M is the Mass of the target, m is mass of electron, I is the irradiance of laser light, ΔE is the bandgap of target material and c is the vacuum speed of light.

The first term is related to the energy gain of the electrons from the electric field, whereas the second term describes the energy transfer from the electrons to the heavy molecules during elastic collisions.

D) Diffusion and Recombination

The decrease of the electron density in the focal volume by electron diffusion can be estimated by approximating the focal volume by a cylinder with radius and length. This leads to the following expression for the diffusion rate per electron

$$g = \frac{\tau \Delta E}{3m} \left[\left(\frac{2.4}{\omega_0} \right)^2 + \left(\frac{1}{z_r} \right)^2 \right] \dots\dots\dots (1.14)$$

z_r is the Rayleigh length and ω_0 is the radius of beam waist. As we are considering ultra short pulses, picoseconds, and below, and plasma diffusion is not operative on these short timescales, but rather occurs long after the pulses have left the interaction region.

CHAPTER 2

LASER INDUCED BREAKDOWN SPECTROSCOPY (LIBS)

2.1 Introduction

Laser induced breakdown spectroscopy (LIBS) is a relatively new version of atomic emission spectroscopy made possible with the invention of the laser. It is also known as laser induced plasma spectroscopy (LIPS). This phenomenon was first reported in 1963 by Maker et al. This analytical technique is based on optical detection of certain atomic and molecular species by monitoring their emission signals from the laser-induced plasma. The LIBS technique has demonstrated a unique versatility: little or no sample preparation, fast, remote and real-time analysis. Efforts for improving its sensitivity are constantly expansion of the ablated vapor cloud in vacuum or into a back ground gas. The first two regimes start with the emergence of the laser pulse and continue until the duration provided form facing new challenging applications.

In the laser-induced breakdown spectroscopy (LIBS) an intense laser beam is focused on the surface of a target which generates a micro plasma. This process is divided in to three regions, (i) interaction of the laser beam with the target material resulting in the evaporation of the surface layers; (ii) interaction of the evaporated material with the incident laser beam resulting in an isothermal plasma formation and expansion; and (iii) anisotropic adiabatic of the laser pulse, whereas the last regime starts after the termination of the laser pulse.

This is schematically shown in figure below

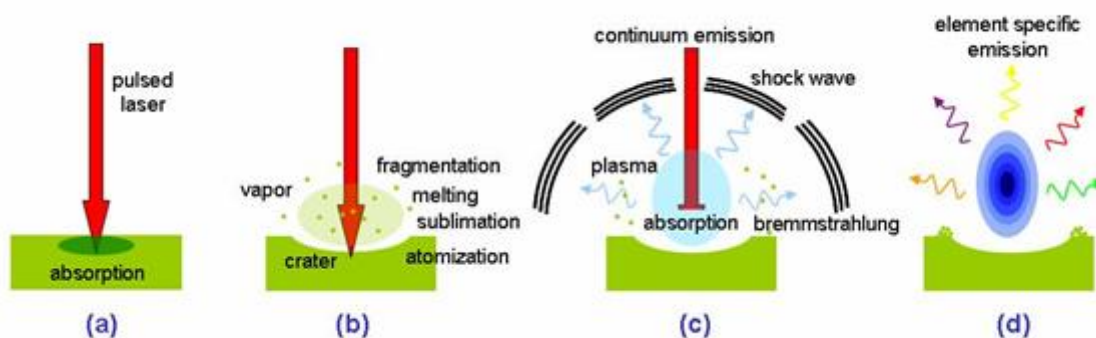


Figure 2.1: Schematic of laser induced breakdown process

When the laser power density exceeds the breakdown threshold value of the solid surface plasma emission occurs. Although different materials have different breakdown thresholds, an optical

plasma is produced when the laser power density exceeds several megawatts per centimeter squared ($10^6 - 10^9 \text{W/cm}^2$). This plasma has been used for sampling, atomization, excitation, and ionization in analytical atomic spectroscopy.

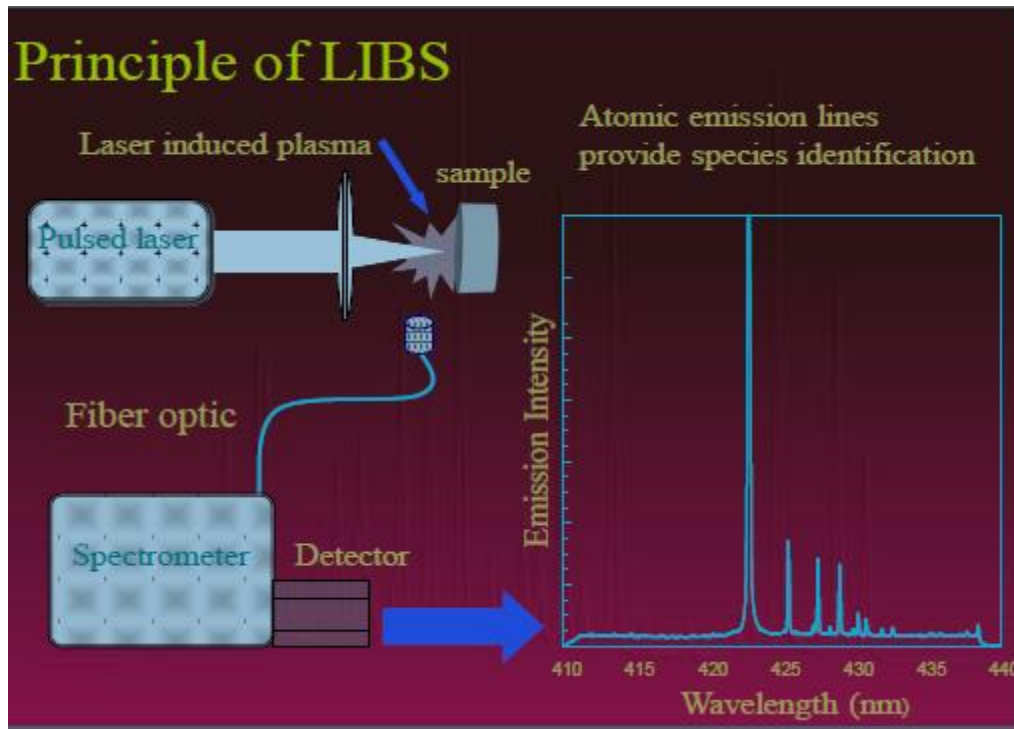


Figure 2.2: Schematic of laser induced breakdown spectroscopy set up.

A typical LIBS system consists of a pulsed laser system and a spectrometer with a wide spectral range and a high sensitivity, fast response rate, time gated detector. This is coupled to a computer which can rapidly process and interpret the acquired data. As such LIBS is one of the most experimentally simple spectroscopic analytical techniques, making it one of the cheapest to purchase and to operate. The LIBS plasma is weakly ionized plasma in which the ratio of electrons to other species is 10%. The formation of laser induced plasma on a metal target in an ambient gas depends on different parameters like laser wavelength, laser power density, surface state and nature, gas pressure and nature, and interaction geometry. Many spectroscopic tools like emission spectroscopy, laser induced fluorescence, absorption spectroscopy, mass spectroscopy, ion probe method, Michelson interferometry etc are used for the characterization of the photo fragmented species in a plasma. Of these the nonrestrictive methods to study the laser plasmas are mass spectrometry and optical emission spectrometry. Optical emission spectroscopic technique is concerned with the light emitted by

electronically excited species in laser induced plasma produced in front of the target surface. Also optical emission measurements are useful for species identification and in situ monitoring during deposition. Useful information about the elemental composition of the target material can be obtained from the analysis of the emissions emanating from the plasma plume.

The laser pulse duration is an important parameter describing its interaction with the material as well as with the plasma. Femtosecond laser beams can induce promising properties which might allow analytical improvements of nanosecond-laser induced breakdown spectroscopy (ns-LIBS). The interesting feature of femto-LIBS is basically due to the specific ablation regime of femtosecond pulses. A pulse duration shorter than the thermal coupling time constant in matter leads to a domination of multiphoton-induced ionization over thermal decomposition, and an expansion of the ejected plasma without further interaction with the laser pulse. The specific properties of femtosecond ablation have been extensively studied for better performance of laser micromachining or microfabrication. Efficient, fast, and localized energy deposition in femtosecond regime allows minimum thermal and mechanical damage of the substrate and a precise material removal. For analysis purposes using LIBS, specific properties of the plasma induced by a femtosecond pulse, allow us to expect an improved sensibility for trace element detection.

2.2 Advantages of Laser Induced Breakdown Spectroscopy

Laser Induced Breakdown Spectroscopy is a popular technique which has been used for a wide variety of applications, such as material analysis, environmental monitoring, forensics, biological identification and even characterization of fossils etc. Additionally, this technique requires little or no sample preparation and can provide simultaneous multi-element analysis. LIBS is an entirely optical technique, therefore it requires only optical access to the specimen. This is of major significance as fiber optics can be employed for remote analyses. And being an optical technique it is non-invasive, non-contact and can even be used as a stand-off analytical technique when coupled to appropriate telescopic apparatus. These attributes have significance for use in areas from hazardous environments to space exploration. Additionally LIBS systems can easily be coupled to an optical microscope for micro-sampling adding a new dimension of analytical flexibility. With specialized optics or a mechanically positioned specimen stage the laser can be scanned over the surface of the specimen allowing spatially resolved chemical analysis and the creation of 'elemental maps'. This is very significant as chemical imaging is becoming more important in all branches of science and technology.

LIBS technique is considered essentially non-destructive or minimally-destructive, and with an average power density of less than one watt radiated onto the specimen there is almost no specimen heating surrounding the ablation site because such a small amount of material is consumed during the process. Due to the nature of this technique sample preparation is typically minimized to homogenization or is often unnecessary where heterogeneity is to be investigated or where a specimen is known to be sufficiently homogeneous, this reduces the possibility of contamination during chemical preparation steps. One of the major advantages of the LIBS technique is its ability to depth profile a specimen by repeatedly discharging the laser in the same position, effectively going deeper into the specimen with each shot. This can also be applied to the removal of surface contamination, where the laser is discharged a number of times prior to the analyzing shot. LIBS is also a very rapid technique giving results within seconds, making it particularly useful for high volume analyses or on-line industrial monitoring.

LIBS has many advantages over conventional Atomic Emission Spectroscopy techniques that use an adjacent physical device (e.g. electrodes, coils) to form the vaporization/excitation source. Some of the advantages of LIBS, like other methods of Atomic Emission Spectroscopy are

- ability to detect all elements,
- simultaneous multi-element detection capability,
- simplicity,
- rapid or real-time analysis,
- the need for little or no sample preparation. This results in increased throughput, greater convenience and fewer opportunities for contamination to occur allows *in situ* analysis requiring only optical access to the sample,
- it has versatile ability to sample gases, liquids, and solids equally well,
- very small amounts of sample (0.1 µg to 1 mg) are vaporized, therefore LIBS can be considered as quasi non-destructive,
- good sensitivity for some elements (e.g. Cl, F) difficult to monitor with conventional AES methods and permits analysis of extremely hard materials that are difficult to digest or dissolve (e.g., ceramics, glasses and superconductors).
- adaptability to a variety of different measurement scenarios,
- the analysis is simple and rapid (ablation and excitation processes are carried out in a single step).

Portable LIBS systems are more sensitive, faster and can detect a wider range of elements (particularly the light elements) than competing techniques such as portable x-ray fluorescence.

2.3 Applications of Laser Induced Breakdown Spectroscopy

LIBS has been applied to various fields such as metallurgy, environmental problems, organic molecules, solution or colloidal phase, combustion processes, nuclear industry, and geology. Among the applications of LIBS, elemental composition analysis of metallurgical samples has been the most popular. Recent applications, however, are more inclined to environmental samples and liquid samples which include biological specimens. The range of potential applications is unequalled by any other analytical technique and is due to its many well known advantages, which include simplicity, lack of sample preparation for the analysis of gases, liquids, and solids, simultaneous multi-element detection, ability to detect high and low z elements, good sensitivity for many elements, only optical access to the target is required standoff analysis capabilities. These advantages permit application of LIBS to real-world analysis needs that cannot be addressed by conventional analytical methods.

The technological developments leading to the emergence of broadband high resolution spectrometers has led LIBS with unique capabilities to extract spectral information microplasmas. It is now possible to detect almost all chemical elements in the periodic table by analyzing the emission in laser generated sparks. Broadband high resolution detection systems enable simultaneous analysis of multiple component elements of targeted samples. LIBS based technologies are rapidly developing. The use of femtosecond laser pulses in LIBS experiments has led to better precision and better reproducibility in emission measurements as compared to the nanosecond pulses. This improvement is attributed to high peak power of laser. Femtosecond lasers consistently create well defined craters and lead to better ablative reproducibility than nanosecond lasers. In contrast to nanosecond pulse the ablation threshold is lower and the energy is more localized in the sample leading to better spatial resolution.

The analysis of single microscopic particles aerosols and cells has received great interest in recent years. A novel feature of LIBS for single particle analysis is its ability to provide elemental mass composition and size data for individual particles .LIBS is the preferred detection and identification technique because of its many characteristic features, including flexibility of point detection and fast real-time response .The fact that LIBS generally requires little-to-no sample preparation, simple instrumentation, and can easily be performed on-the-field in hazardous industrial environments in real-

time, it is a very attractive analytical tool. The following are a few examples of real life applications, where LIBS is successfully used:

- Express-analysis of soils and minerals (geology, mining, construction)
- Exploration of planets (such as projects using LIBS for analyzing specific conditions on Mars and Venus to understand their elemental composition)
- Environmental monitoring (Real-time analysis of air and water quality, control of industrial sewage and exhaust gas emissions)
- Biological samples (non-invasive analysis of human hair and teeth for metal poisoning, cancer tissue diagnosis, bacteria type detection, detection of bio-aerosols and bio-hazards, anthrax, airborne infectious disease, viruses, sources of allergy, fungal spores, pollen). Replacing antibody, cultural, and DNA types of analysis
- Archeology (analysis of artifacts restoration quality)
- Architecture (quality control of stone buildings and glasses restoration)
- Army and Defense (detection of biological weapons, explosives, backpack-based detection systems for homeland security)
- Forensic (gun shooter detection)
- Combustion processes (analysis of intermediate combustion agents, combustion products, furnace gases control, control of unburned ashes)
- Metal industry (in-situ metal melting control, control of steel sheets quality, 2D mapping of Al alloys)
- Nuclear industry (detection of cerium in U-matrix, radioactive waste disposal)

CHAPTER 3

INSTRUMENTATION FOR LASER INDUCED BREAKDOWN SPECTROSCOPY AND TIME EVOLUTION STUDIES

3.1 Introduction

The technique for direct detection of the spectral emission of a plasma plume formed above a sample surface by incident laser radiation is referred as LIBS which has a huge potential for analysis of environmental samples and other applications. In this chapter components used for LIBS and Dynamics studies are explained in detail.

A typical LIBS apparatus is shown in the figure 3.1.

The LIBS setup generally include,

1. The pulsed Laser system that generates the powerful optical pulses.
2. The focusing system of mirror and lens that directs and focuses the laser pulse on the target sample.
3. Sample chamber and a target holder.

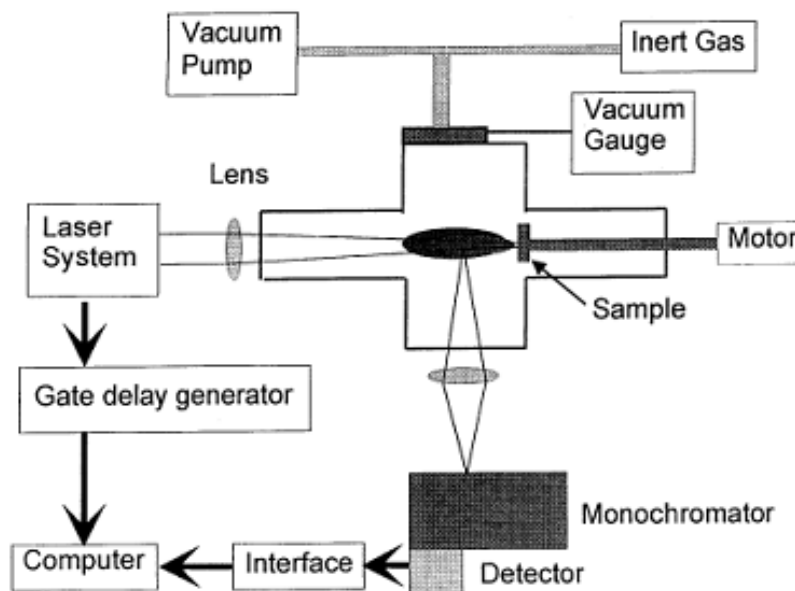


Figure 3.1: Laser Induced Breakdown Spectroscopy setup

4. The light collection system that collects the spark light and transport the light to the detection system.
5. Detection system consisting of spectrometer, Photomultiplier tube, CCD, ICCD to study the plasma emission spectrum
6. Computer and electronics to gate the detector, store the spectrum etc.

A typical setup for time-resolved LIBS is shown in Figure 3.1. The solid target which we have used was Copper with 99.9% purity. When an intense pulsed laser beam is focused onto the target which is kept inside the vacuum chamber, breakdown of the sample occurs, which eventually results in the creation of spark, frequently called laser-induced plasma, and rapidly heats the sample region to extremely high temperature. The light emitted from the plasma was collected and analyzed using iHR320 imaging spectrometer interfaced with CCD camera or Photomultiplier Tube.

3.2 Laser System

Two types of laser systems with different intensity regime was used for the laser induced plasma spectroscopy and dynamics of copper target. They are Q-switched neodymium doped yttrium aluminum garnet (Nd: YAG) laser and Titanium Sapphire laser.

A) Nd:YAG laser(Quanta Ray Spectra-Physics)

The Nd:YAG laser(Quanta Ray Spectra Physics) used for plasma generation is pulsed laser system emitting at a wavelength of 1064nm, delivering an energy up to 600 millijoules per pulse with pulse width 7ns and repetition rate 10Hz. The gain medium is the YAG crystal doped with around 1% neodymium by weight, which is optically pumped by a flash lamp. The triply ionized neodymium typically replaces yttrium in the crystal structure of the yttrium aluminum garnet (YAG), since they are of similar size. The Quanta Ray Nd:YAG laser system comprises of laser head, controller and power supply. The laser oscillator has two pump chambers assembled with one flash lamp on each chamber for high power. The 1064 oscillator is typically followed by optical harmonic generation (HG) stage that can be set to generate 532,355 or 266nm output wavelengths. The HG is followed by a pair of dichroic mirrors that reflect the desired harmonic as laser output, while transmitting the undesired wavelengths in to a beam dump. The controller employs conventional knobs and switches for setting and controlling the various system parameters. The laser comprising of an active media and resonator

will emit a pulse of laser light each time the flash lamp fires. The pulse duration will be long and its peak power will be low. When a Q switch is added to the resonator to shorten the pulse the output peak power will increase.



Figure 3.2: Nd YAG laser system

A large population of excited Neodymium ions can build up in the YAG rod .If the oscillation is prevented while the population inversion builds and if the store energy can be released quickly, the laser emits a short pulse of high intensity light. To do this an electro optic device (Q switch) is added to the cavity which introduces high cavity loss and prevents oscillation. This allows the energy to build up. It is then quickly switched to a very low state that allows oscillation to occur and the cavity dumps the energy in the form of a light pulse. The Q switch comprises of a polarizer, quarter wave plate and pockels cell. During Q switch operation, the flash lamp excites the Nd ions for approximately $200\mu\text{s}$ to build up a large population inversion. At the point of maximum population inversion, a fast voltage pulse applied Pockels cell changes the Q-switch from high to low loss. This results in a short pulse of high peak power. The high peak power of Q switched pulses permit frequency conversion in nonlinear crystals like Potassium dideuterium phosphate (KDP).In the simplest case, the 1064nm Nd:YAG fundamental interacts with the crystal to produce a secondary wave with half the fundamental wavelength.

B) Ti: sapphire Laser

For femtosecond laser interaction with the target we have used a Ti Sapphire laser (Tsunami Spectra-Physics) which produces up to 10mJ of energy at 800nm with 100 femtosecond pulse width and repetition rate of 10Hz. Titanium-doped sapphire (Ti: sapphire) is a solid-state laser medium capable of tunable operation over a broad range of near infrared (IR) wavelengths. The mode locked Tsunami laser uses this laser medium and, with properly chosen optics, delivers continuously tunable output over a broad range of near IR wavelengths: from 690 nm to 1080 nm.

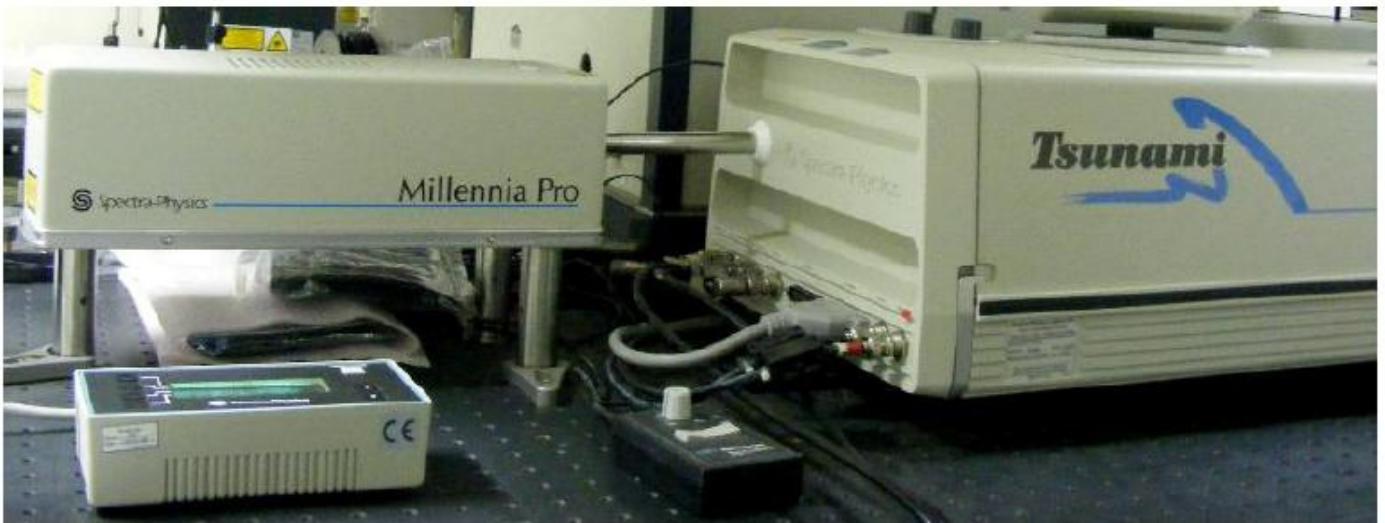


Figure 3.3: The tsunami oscillator with Millennia Pump Laser

A Ti:sapphire laser is usually pumped with another laser with a wavelength of 514 to 532 nm, for which argon-ion lasers (514.5 nm) and frequency-doubled Nd: YAG, Nd: YLF, and Nd:YVO lasers (527-532 nm) are used. Here energy for the lasing process (the “pump” energy) is supplied by a Millennia® series, continuous wave (CW), diode-pumped, solid-state laser which provides a 5.2W of 532 nm to Tsunami. The Tsunami acousto-optic modulator (AOM) ensures reliable mode locked operation at laser start-up. It also allows the laser to operate for extended periods without dropouts or shut-downs associated with standard passively mode-locked systems. The AOM is driven by a regeneratively derived RF signal.

C) Ti: Sapphire chirped pulse amplifier

A regenerative “chirped pulse amplifier” is added to the system for obtaining high energy ultrafast pulses. In the CPA technique, the pulse to be amplified is first stretched in time by a large factor (typically 10,000) in order to reduce the peak power. This pulse can be then safely amplified, and

after amplification, can be compressed back nearly to the original input pulse width. In titanium sapphire amplifier (TSA 10, Spectra Physics), the 100 fs pulses from the femtosecond oscillator are sent to a pulse stretcher, which broadens the pulse to about 300 ps width. Using an electro optic modulator an individual pulse is selected from the 82MHz pulse train and is seeded into a regenerative cavity, which contains an optically pumped Ti: sapphire crystal.

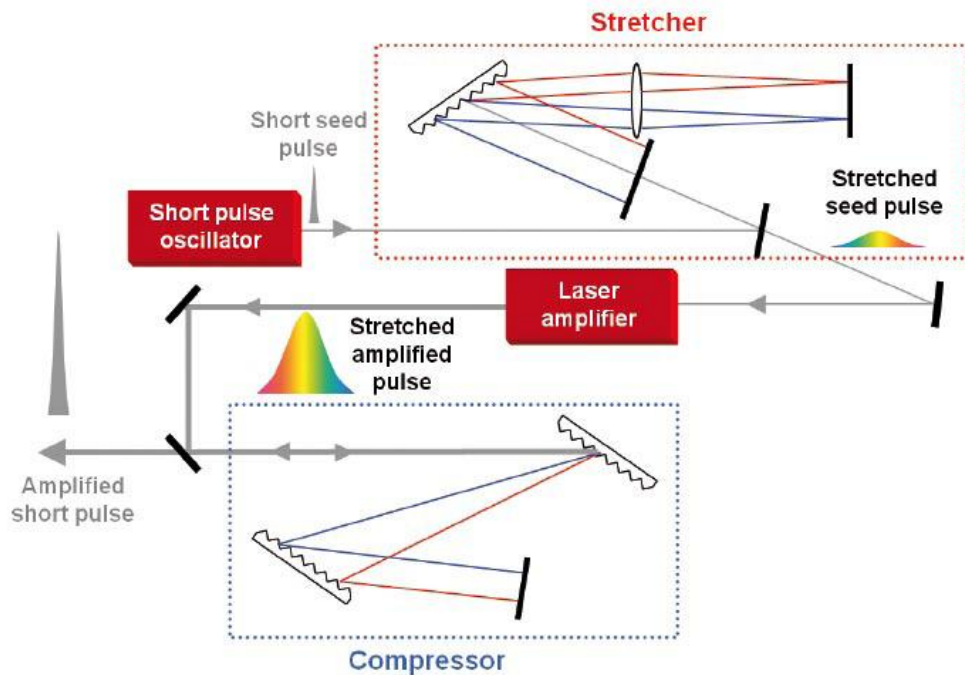


Figure 3.4: Schematic of a chirped-pulse amplification-based laser system.

The regenerative amplification will confine, by polarization, a single pulse (selected from a mode-locked pulse train), amplify it to an appropriate energy level and then “cavity dump” the output. The pulse after several round trips, gains sufficient energy and is reflected out of the cavity using an electro-optic switch. The cavity dumped pulse is then fed to a double-pass linear amplifier for further amplification. The amplified pulse is then sent to a grating compressor, which compresses the pulse back to the original 100 fs width. The TSA-10 generates 100 fs pulses of 10 mJ energy at a repetition rate of 10Hz.

3.3 Sample Chamber

A sample chamber is an essential part for the plasma generation for most of the experiments performed by LIBS at laboratory scale. This is due to the reason that experiments by LIBS can be

performed at various ambient gas pressures by introducing different gases in the chamber or in vacuum. Sample chamber can be evacuated by a rotary mechanical vacuum pump. This sample chamber was specially designed for producing high vacuum inside it and was made of stain less steel. The sample chamber was constructed with the provisions of introducing various gases in to it and evacuating whenever required. The target sample inside the chamber can be rotated by a step motor with a sample holder to get the fresh surface for each LIBS measurement .A vacuum gauge is used to measure the pressure inside the vacuum chamber. We have used Maxi Gauge TPG 256 a vacuum gauge which is a 6-port total pressure measurement and control unit for vacuum compact gauges like Pirani Gauge. The Pirani gauge can be used for measuring a vacuum range of 760 torr to 3.75×10^{-4} torr. Lower pressures are measured by using a cold cathode gauge, which has a measuring range of 7.5×10^{-3} Torr to 1.5×10^{-9} Torr.

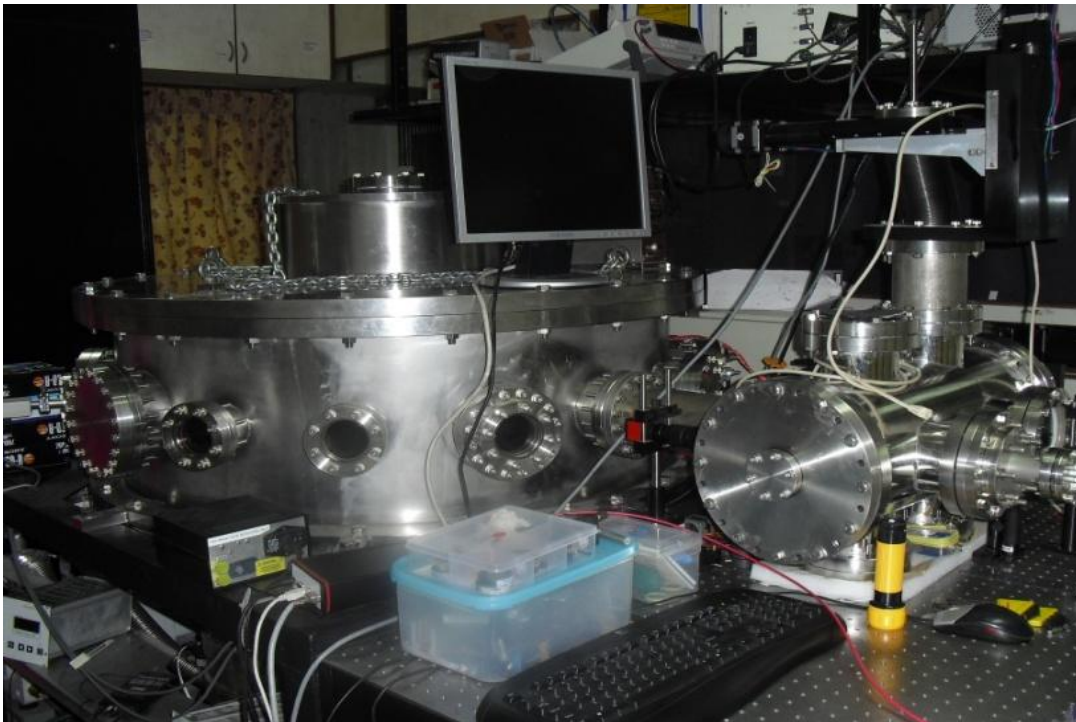


Figure 3.5: Vacuum chamber used for LIBS experiment

Vacuum quality is subdivided into different pressure ranges as Rough vacuum ($760-10^{-3}$ torr). High vacuum ($10^{-4} - 10^{-8}$ torr), and Ultrahigh vacuum (10^{-9} to 10^{-12} torr). Rough vacuum can be obtained by using mechanical pumps like rotary vane pumps and high vacuum can be attained by using turbo molecular pumps in series with the mechanical pump. For ultrahigh vacuum gyro pumps or ion pumps in series with the mechanical pump can be used.

3.4 Imaging and Detection

The radiation emitted by the plasma was collected and focused on to the slit of the spectrometer for detection by two convex lenses and a mirror which is placed right angle to the direction of the laser beam. The beam collimated by the first lens is focused by the other and is allowed to fall on the slit of the spectrometer by using a mirror.

a) Spectrometer

A spectrometer is an instrument used to measure properties of light over a specific portion of the electromagnetic spectrum, typically used in spectroscopic analysis to identify materials. Simultaneous recording of spectra at multiple locations in plasma can provide critical information about spatially varying phenomena. We have used iHR320 imaging spectrometer (HORIBA Jobin Yvon) for spectroscopic analysis. It is Czerny-Turner spectrometers, which has enhanced capabilities for use with a CCD or Photomultiplier tube.

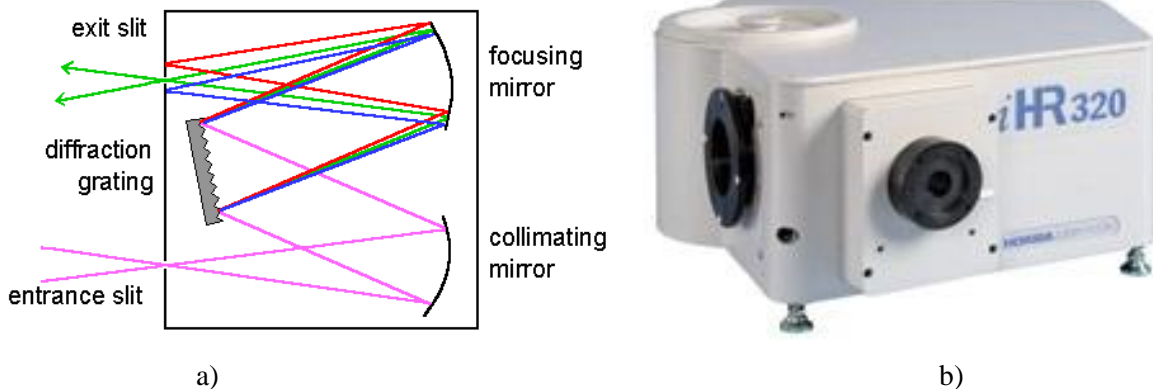


Figure 3.6: a) Schematic of grating monochromator, b) iHR 320 spectrometer (Horiba Jobin Yvon).

The radiation emitted by the plasma was collected and focused on to the entrance slit of the spectrometer. The slit is placed at the effective focus of a curved mirror so that the light from the slit reflected from the mirror is collimated (focused at infinity). The collimated light is diffracted from the grating and then is collected by another mirror which refocuses the light, on the exit slit. At the exit slit of the spectrometer a compact CCD detector or a photomultiplier tube is interfaced for recording many lines simultaneously.

b) Synapse CCD Detector

Synapse CCD detectors is designed to interface with all HORIBA Jobin Yvon spectrometers and provide highly sensitive detection for any experiment. The Synapse CCD uses a high-speed USB 2.0 interface which allows for a fast, simple computer connection. It quickly connects to SynerJY software for easy detector and spectrometer control and data acquisition. Some of the features of Synapse CCD detector like flexible triggering, signal linearity, high sensitivity, and low noise make it complete solution for modern spectroscopic measurements. The low-noise amplifiers are located next to the CCD sensor to minimize any noise from the external environment.



Figure 3.7: Synapse CCD Detector

c) Photomultiplier Tube

The photomultiplier is a very versatile and sensitive detector of radiant energy in the ultraviolet, visible, and near infrared regions of the electromagnetic spectrum. Photomultipliers are constructed from a glass envelope with a high vacuum inside, which houses a photocathode, several dynodes, and an anode. Incident photons strike the photocathode material, which is present as a thin deposit on the entry window of the device, with electrons being produced as a consequence of the photoelectric effect. These electrons are directed by the focusing electrode toward the electron multiplier, where electrons are multiplied by the process of secondary emission. The electron multiplier consists of a number of electrodes called dynodes. Each dynode is held at a more positive voltage than the previous one. The electrons leave the photocathode, having the energy of the incoming photon minus the work function of the photocathode.

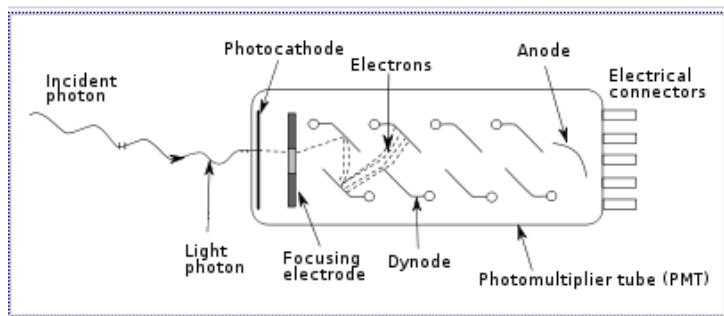


Figure3.8: Schematic representation of a photomultiplier tube and its operation

As the electrons move toward the first dynode, they are accelerated by the electric field and arrive with much greater energy. Upon striking the first dynode, more low energy electrons are emitted, and these electrons in turn are accelerated toward the second dynode. The geometry of the dynode chain is such that a cascade occurs with an ever-increasing number of electrons being produced at each stage. Finally, the electrons reach the anode, where the accumulation of charge results in a sharp current pulse indicating the arrival of a photon at the photocathode.

d) ICCD Camera (4 Picos- Stanford Computer Optics. Inc)

4 Picos is most compact intelligent ICCD pico-fast camera system. An image intensified high speed camera basically consists of a high performance CCD camera and an image intensifier that is mounted in front of it. The incoming light is first amplified by the image intensifier. The intensified image is then transmitted from the intensifier's phosphor screen and projected onto the CCD sensor by means of a coupling lens. Main highlights of 4 picos ICCD camera are; they enable single photon detection, the Dynamic range of this ICCD range up to 32bit using a Dynamic Range Expansion System.

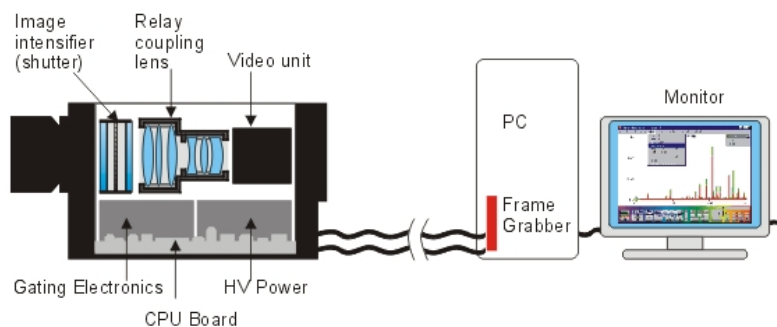


Figure 3.9: Schematic showing the working of ICCD

Spectral sensitivity is from UV to NIR region. It offers a high resolution of 1360x1024 pixels. We have used ICCD in our experiment to study the temporal evolution of plasma plume at different time instants.

e) Tektronix –Digital Phosphor Oscilloscope

The photomultiplier signal was measured with Tektronix Digital Phosphor Oscilloscope 7354. This is a fast oscilloscope which provides exceptional performance in signal acquisition and analysis. It possesses high sampling rate up to up to 40 GS/s on one channel and up to 10 GS/s on all four channels.



Figure 3.10: Tektronix –Digital Phosphor Oscilloscope

For Better Low-frequency Measurement Accuracy User-selectable Bandwidth Limit filters are there. The fast acquisition mode enabled by Tektronix DPX acquisition technology facilitates analysis of dynamics of signal and capture of infrequent events.

CHAPTER 4

LASER INDUCED BREAKDOWN SPECTROSCOPY STUDIES OF COPPER USING NANOSECOND AND FEMTOSECOND LASER PULSES

4.1 Introduction

Laser- induced plasmas of metal alloys have different attractive and important applications, e.g., material processing, thin film deposition, etc. and thus research in this field are of great interest. The metal target that we have used for our work is pure copper (99.9%). The element of copper being a good metal has vast applications in electronic and electric engineering. Due to the widespread use and laser processing of copper, makes it useful for research in major industries such as thin-film deposition by laser ablation, nanotechnology etc.

The interaction of femtosecond laser with materials is considerably different from that of nanosecond laser pulses. In this chapter spectroscopic study of copper plasma produced by the fundamental harmonic, 1064nm of Nd YAG laser and Ti Sapphire (800nm) femtosecond laser is given. The laser-induced plasma is a light-emitting micro-source and it is expected that the lines and their intensities observed are indicative of the elemental composition of the sample. To establish a quantitative relationship between the emission spectrum and plasma properties, two parameters are introduced: the plasma temperature T_e and the electron density n_e .

4.2 Experimental Setup

In the present work femto second and nanosecond laser interaction with the copper target is studied. For this we have used two types of laser systems with different intensity. For femto second laser interaction with the copper target output from a femto-second oscillator (Tsunami - Spectra-Physics) with chirped pulse amplifier (TSA10 - Spectra Physics), capable of generating 100 fs pulses of 10 mJ energy and the beam diameter of about 8mm is focused onto the target by using a 50cm lens. The schematic diagram for the experiment is as shown in figure (4.1). The target is kept inside a vacuum chamber. The target is mounted on a sample holder which can be moved by a step motor to get the fresh surface for each LIBS measurement. The pressure inside the vacuum chamber can be varied.

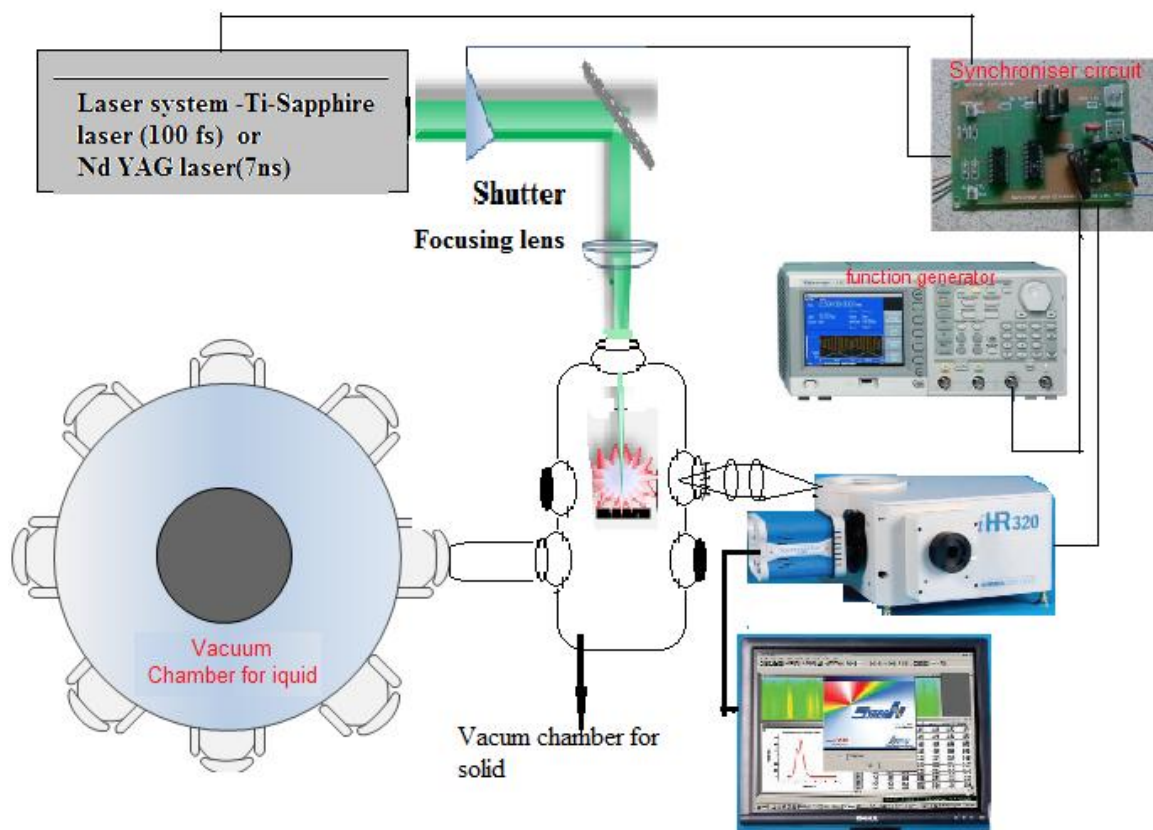


Figure 4.1: Schematic diagram for the laser induced plasma from the solid target at different background pressure

Rough vacuum ($760 \cdot 10^{-3}$ torr) can be obtained by using mechanical pumps like rotary vane pumps and high vacuum (10^{-4} - 10^{-8} torr) can be attained by using turbo molecular pumps in series with the mechanical pump. A vacuum gauge (Pirani Guage) was used to measure the pressure in a vacuum. In this experiment measurements are taken at different pressure from 760 torr to 10^{-6} torr. The plasma emission was collected and focused on to the slit of the spectrometer for detection by two convex lenses and a mirror which is placed right angle to the direction of the laser beam. This is allowed to fall on the slit of the iHR320 imaging spectrometer (HORIBA Jobin Yvon). A CCD detector (Synapse) interfaced to the spectrometer is used to record the emission profile on the computer and this was analyzed by using Synergy software.

The experiment is repeated for three times under identical experimental conditions. Same experimental setup and conditions are used for LIBS studies on copper using nanosecond laser except the laser source. Here we have used fundamental harmonic i.e. 1064 nm from a Q switched Nd: YAG laser which produces nanosecond pulse of pulse width 7 ns at 10 Hz repetition rate.

4.3 Results and Discussions

In this chapter the emission spectra of both femtosecond and nanosecond laser produced copper plasma at different background pressure are studied. Intensities of the femtosecond and nanosecond laser used for laser induced breakdown of copper are $1.27 \times 10^{15} \text{W/cm}^2$ and $4.82 \times 10^{10} \text{W/cm}^2$ respectively. The sample emission covering from a range of 350nm-700nm was detected using iHR 320 spectrometer which is interfaced with CCD detector. The emission spectrum is used to calculate the plasma parameters.

a) Emission Studies

The laser ablation process can be classified into three regimes: evaporation of the target material, interaction of the evaporated cloud with incident laser beam resulting in cloud heating and plasma formation, and expansion and rapid cooling of the plasma. Observations were made of the plasma created by the interaction of the laser beam with the target in a direction perpendicular to that of the laser beam. Plasma produced by a high intensity laser pulse expands normal to the target surface due to shock waves. In the present work, we have produced copper plasma with two intensity regimes one a femto-second oscillator (Tsunami - Spectra-Physics) with chirped pulse amplifier (TSA10 – Spectra-Physics) and the other Q-switched Nd:YAG laser with its fundamental 1064 nm. In the first set of experiments, the output from femtosecond laser system (800 nm) with 10 mJ pulse energy and 100fs pulse width was focused on the copper target. The emission spectra of the plasma produced at the surface of the copper target is recorded. Experiment was repeated for different pressure varying from 760 torr to 10^{-6} torr. In the second set of experiments the femtosecond laser system is replaced by Q-switched Nd:YAG laser (fundamental 1064 nm) with 60mJ energy and 7ns pulse width. Experiment is then repeated with identical conditions as in the first case.

Figure (4.2) and figure (4.3) shows the obtained emission spectrum of femtosecond and nanosecond laser produced Cu plasma covering from 350nm–700nm at a pressure of 1 torr in air atmosphere, which consists of atomic and ionic Cu lines. The plasma emission spectra was recorded by iHR 320 spectrometer interfaced with a Synapse CCD detector. The spectral analysis was done using Synergy Software. The emission spectrum of copper revealed the formation of neutral atoms and singly charged ions.

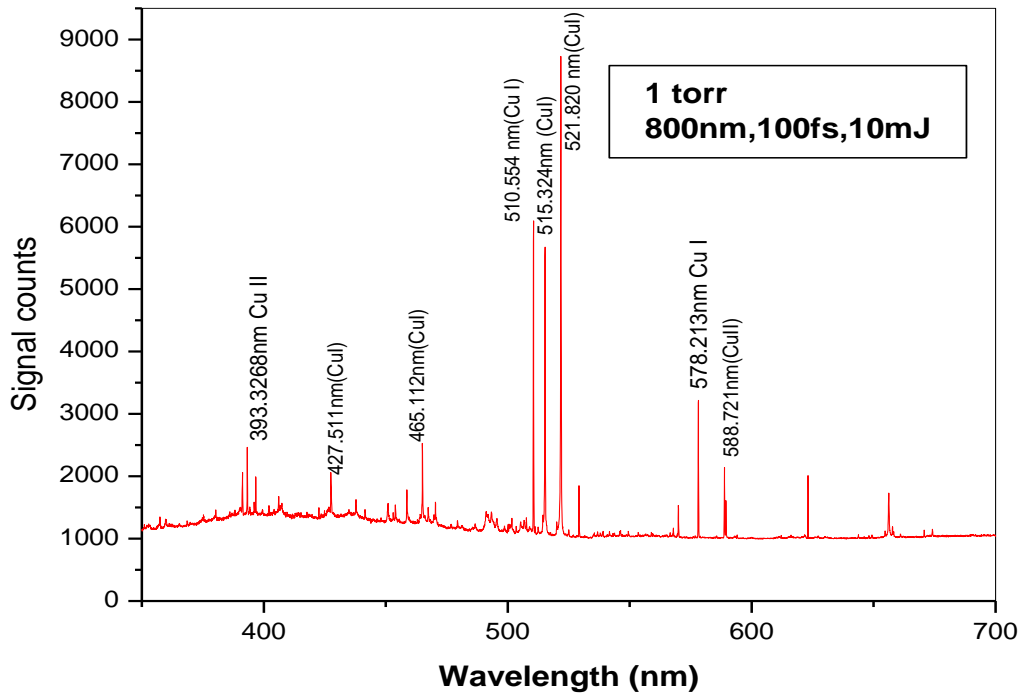


Figure 4.2: The emission spectra of femtosecond laser produced copper plasma at 1 torr

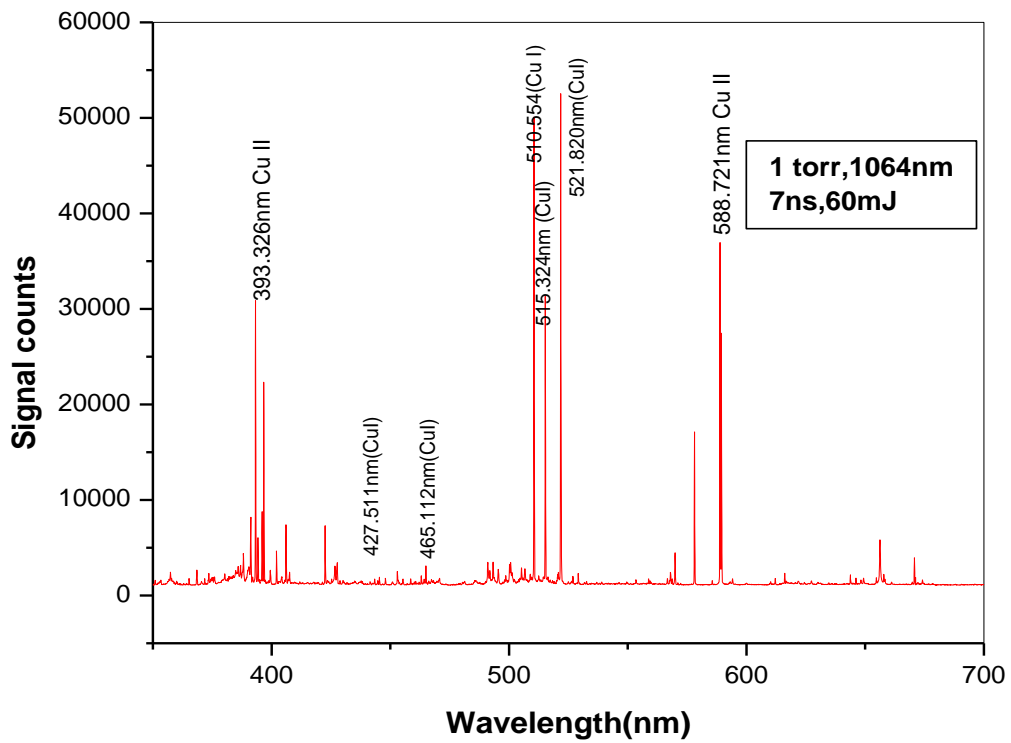


Figure 4.3: The emission spectra of nanosecond laser produced copper plasma at 1 torr

The emission spectrum of copper plasma using femtosecond laser is shown as in the figure (4.2). The intensity of Cu I lines are more pronounced at transitions $[4p\ ^2P-4d^2D]$ i.e. 515.324, $[4p\ ^2P-4d\ ^2D]$ i.e. 521.820 and $[4s^2\ ^2D-4p\ ^2P]$ i.e. 510.554nm while Cu II lines such as $[4p\ ^1F-6d\ ^3D]$ i.e.393.326nm and $[5p\ ^3P-5d\ ^3D]$ i.e. 588.721 nm have relatively low intensity. No Cu III lines were detected in these regions. Similar to the femtosecond LIBS result for copper, the emission spectra of nanosecond laser produced show two strongest peaks in the spectrum at wavelengths 510.581nm and 521.820nm both correspond to Cu I. The intensities of Cu II lines at 393.326nm and 588.721nm have high intensities relative to the Cu II lines in the femtosecond regime.

The identification of atomic and ionic Cu lines was done by using PLASUS Specline software. The PLASUS Specline software has extensive database for atoms, ions and molecules.

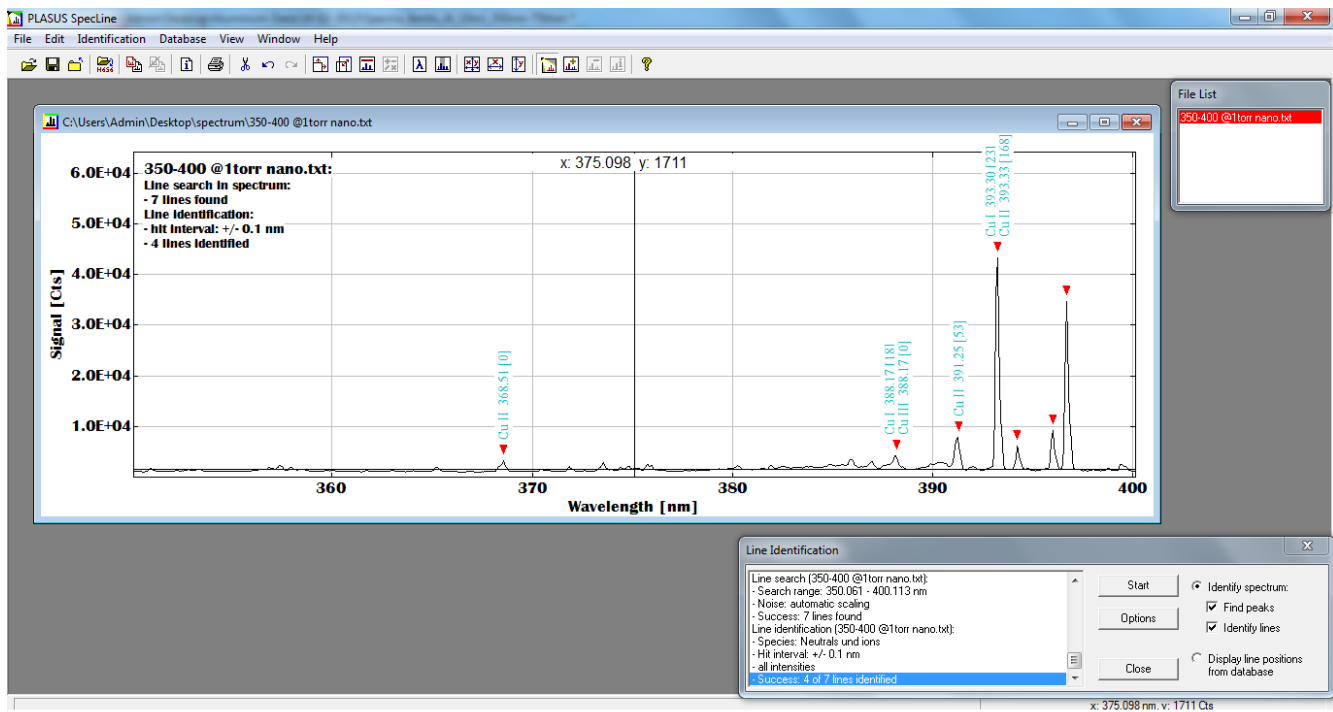


Figure 4.4: Identification of lines using Plasus Specline software

When a high power laser pulse is focused on a solid target, hot plasma formed above the surface expands at supersonic speed by driving a shock wave into the surrounding atmosphere. During this interaction, energy is transferred into the ambient atmosphere through several processes such as, shock heating, thermal conduction, radiative emission and ion recombination. The extent of this interaction depends on the energy, pulse duration and the wavelength of the laser used as well as, composition and the condition of this ambient atmosphere. By comparing the femtosecond and nanosecond measurements it is observed that the emitted spectral intensity is more in the nanosecond regime. This is because majority of photons from femtosecond lasers reach the surface before the laser plasma

develops, while with the nanosecond pulse lasers, a significant portion of the photons are able to interact with the expanding plume. At reduced pressures, a plasma generated with a nanosecond pulse is expanding in a less dense atmosphere, which results in a less dense shock wave. The reduced density in the shock wave results in reduced plasma shielding; thus, allowing more photons to reach the sample. Increasing the number of photon interacting with surface results in increased sample ablation, which can also lead to a more intense spectrum.

b) Determination of electron temperature and number density of plasma

The key parameters of laser ablated plume are electron density and electron temperature. The obtained spectra are helpful in extracting the electron temperature and density of the plasma. The factors that influence the emitted intensity by plasma are the number density of emitting species (ions and neutrals), electron density and temperature. These parameters are also responsible for different excitation and ionization processes occurring in laser-produced plasma. Many methods have been described for determining the plasma temperature based on the absolute or relative line intensity (line pair ratio or Boltzmann plot), the ratio of line to continuum intensity, etc. Depending on the experimental conditions, one of these methods may be more suitable than others. Provided that the Local Thermodynamic Equilibrium (LTE) hypothesis is fulfilled, the plasma temperature can be calculated from the intensity ratio of a pair of spectral lines originating in different upper levels of the same element and ionization stage. Boltzmann's law could be applied to two spectral lines, of intensities I_1 and I_2 and the electronic temperature T_e was obtained through their intensity ratio

$$\frac{I_1}{I_2} = \frac{A_2 \lambda_1 g_2}{A_1 \lambda_2 g_1} e^{-(E_2 - E_1)/k_B T_e} \dots\dots\dots (4.1)$$

with A_j the Einstein coefficient of the j transition, λ_j the wavelength of emission of this transition, g_i the statistic weight, and E_j the energy of the j state. When selecting a line pair, it is advisable to choose two lines as close as possible in wavelength and as far apart as possible in excitation energy. This is to limit the effect of varying spectral response of the apparatus, as well as to minimize the sensitivity to small fluctuations in emission intensity.

The emitted spectral line intensity is a measure of the population of the corresponding energy level of a certain species in the plasma. Under the assumptions that the plasma is both in Local Thermodynamic equilibrium and optically thin, if we have information on the intensity emitted from several excited levels, we can then determine the temperature which is responsible for the observed

population distribution. The condition that the atomic and ionic states should be populated and depopulated predominantly by electron collisions, rather than by radiation, requires an electron density which is sufficient to ensure the high collision rate. The corresponding lower limit of the electron density is given by McWhirter criterion

$$N_e \geq 1.6 \times 10^{12} T^{1/2} \Delta E^3 \dots\dots\dots (4.2)$$

where T (K) is the plasma temperature and ΔE (eV) is the energy difference between the states, which are expected to be in local thermodynamic equilibrium (LTE).

The relevant spectroscopic parameters for the transitions of the laser-produced copper plasma used in calculations have been taken from the NIST Atomic spectra database and Plasus Specline and are listed in table (4.1).

Transition Wavelength(nm)	Transitions	Statistical weight		Transition probabilities(A _{ji} in s ⁻¹)	Energy of the upper level E _j (eV)
		g _i	g _j		
427.511	4p ¹ 4P -5s ¹ 4D	6	8	3.45E+7	7.74
465.112	4p ¹ 4F -5s ¹ 4D	10	8	3.8E+7	7.74
510.554	4s ² 2D -4p 2P	6	4	2E+6	3.82
515.324	4p 2P -4d ² D	2	4	6E+7	6.19
521.820	4p 2P -4d ² D	6	6	7.5E+7	6.19
578.213	4s ² 2D -4p ² P	4	2	1.65E+6	3.79

Table 4.1: Spectroscopic parameters of the neutral Copper lines (From the NIST standard data)

For femtosecond laser produced copper plasma the temperatures at different ambient pressures are calculated from the ratio of intensities of two neutral copper lines 510.554nm and 521.820nm. In the case of nanosecond laser produced copper plasma temperature calculation was done from the ratios of intensities of two neutral copper atom at 465.112nm and 578.213nm. Table 4.2 and 4.3 gives calculated plasma parameters.

Pressure (torr)	Temperature (K)	Number Density(cm⁻³)
2E-6	18074	2.86x10 ¹⁵
2E-3	18215	2.874x10 ¹⁵
5E-2	17353	2.804x10 ¹⁵
2E-1	18868	2.92x10 ¹⁵
1	16990	2.775x10 ¹⁵
10	18420	2.889x10 ¹⁵
20	20409	3.041x10 ¹⁵
50	21477	3.12x10 ¹⁵
100	19847	3.001x10 ¹⁵
200	17779	2.83x10 ¹⁵
760	15695	2.66x10 ¹⁵

Table 4.2: Plasma parameters (temperature and number density) calculated from the emission spectra of femtosecond laser produced copper plasma

Pressure(torr)	Temperature(K)	Number Density(cm⁻³)
5E-2	29638	1.09x10 ¹⁵
1	21031	9.16x10 ¹⁴
10	30330	1.1x10 ¹⁵
20	26774	1.03x10 ¹⁵
50	36278	1.2x10 ¹⁵
100	42950	1.3x10 ¹⁵
200	34822	1.17x10 ¹⁵
760	36144	1.201x10 ¹⁵

Table 4.3: Plasma parameters (temperature and number density) calculated from the emission spectra of nanosecond laser produced copper plasma

The emission spectra, electron temperature and density are found to be significantly influenced by the ambient atmosphere. The addition of an ambient gas enhances the emission from all species. The relative enhancement depends on the nature of the gas, gas pressure and also the excitation energy of the electronic transition responsible for the line. The interaction of femtosecond laser pulses with materials is substantially different from that of nanosecond laser pulses, and offers a number of advantages that have been extensively documented for micromachining applications. Improvements in material removal such as increased reproducibility, reduced material deposition around the ablation area, and a smaller heated volume around the ablation region have motivated the initial studies that used femtosecond lasers for laser-induced breakdown spectroscopy (LIBS), an analytical technique based on the spectral analysis of optical emission from laser-induced plasma.

c) Effect of laser energy

The nature and characteristics of laser-induced plasma strongly depend on the laser irradiance. The size, temperature and hence the extent of ionization is very much dependent on the laser pulse energy. This laser pulse energy is the source of energy for evaporation, atomization and ionization of the target when it is focused inside the sample chamber.

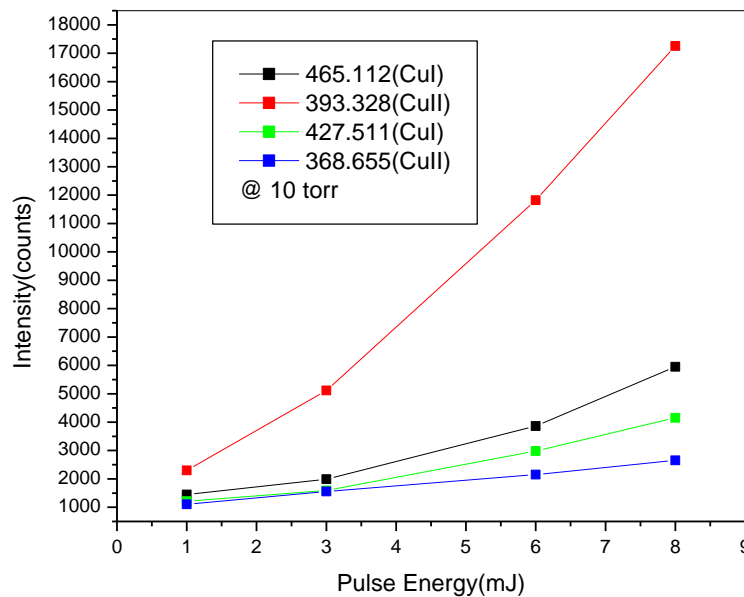


Figure 4.5: Variation of emission intensity with different pulse energy at 10 torr ambient pressure

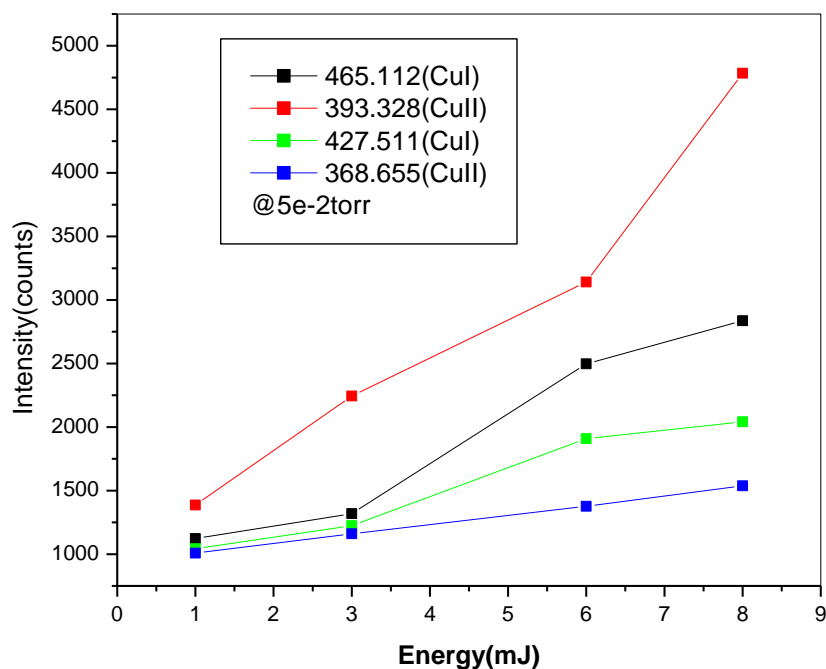


Figure 4.6: Variation of emission intensity with different pulse energy at 1 torr ambient pressure

Figure(4.5 and 4.6) shows the emission spectra of the copper sample for different values of laser energy 1mJ, 3mJ, 6mJ and 8mJ at two different background pressures 10 torr and 5E-2 torr. Emission intensities of two neutral copper atoms at wavelengths 465.112nm ($4p^1 4F - 5s^1 4D$) and 427.511nm ($4p^1 4P - 5s^1 4D$) and two singly ionized copper atoms at wavelengths 368.655nm ($5p^2 D - 6d^2 F$) and 393.328nm ($4p^1 F - 6d^2 F$) were plotted. It was observed that as laser energy increases from 1mJ to 8mJ the intensity of the emission lines also increases at 10 torr and 5E-2 torr background pressure.

CHAPTER 5

TIME-RESOLVED SPECTROSCOPIC STUDY OF FEMTOSECOND LASER INDUCED COPPER PLASMA

5.1 Introduction

Time-resolved spectroscopy is the study of dynamic processes in materials or chemical compounds by means of spectroscopic techniques. Most often, processes are studied that occur after illumination of a material, but in principle, the technique can be applied to any process that leads to a change in properties of a material. Laser Induced Breakdown Spectroscopy is a promising technique for obtaining spectrochemical information from sample locations where it is difficult to place electrodes or extract samples. LIBS can also sample species directly in air or a carrier gas, eliminating sample preparation.

The principal factors influencing the nature of interaction between laser radiation and solid target are duration, wave length, power density of the laser pulse, laser light absorption processes and ambient pressure as well as physical and chemical properties of the target. The dynamics of the plume produced in laser ablation processes is also of considerable interest in understanding the physics of plasma. Theoretical and experimental investigations are actively in progress in order to obtain accurate knowledge of all the physical processes involved in the ablation processes and the dynamics of laser induced plasma (LIP). Most of the above studies reported are carried out by using conventional Langmuir probes and typical investigation techniques of atomic and molecular physics, such as optical emission and absorption spectroscopy. This chapter deals with information on the laser Induced Plasma generation from copper (99.9% pure) metal target by femtosecond laser metal ablation.

5.2 Experimental Setup

A LIBS system typically consists of short pulse laser to generate plasma, a spectrometer for detection and analysis of the plasma light, optical components such as mirror and lens, and a computer. A vacuum chamber is added to analyze plasma characteristics in different pressure regimes. The output from a femto-second oscillator (Tsunami - Spectra-Physics) with chirped pulse amplifier (TSA10 – Spectra-Physics), capable of generating 100 fs pulses of 10 mJ energy and the beam diameter of about

8mm is focused onto the target surface inside of a vacuum chamber by using a lens of focal length 50cm . Single shot was applied to the experiment and it was repeated 5 times in each case. The emitted light from the plasma was collimated on the entrance slit of iHR320 imaging spectrometer which isolates the specific lines. Photomultiplier tube is placed behind the slits as detectors, which produce a photo current proportional to the intensity of the incident radiation.PMT signal was monitored using a digital phosphor oscilloscope. The triggering electronic circuit synchronizes the laser with the detector. The laser light reflected from the target is detected using a photo detector, the output of which is used for triggering the fast oscilloscope. The experimental setup for the time resolved study is shown in figure 5.1.

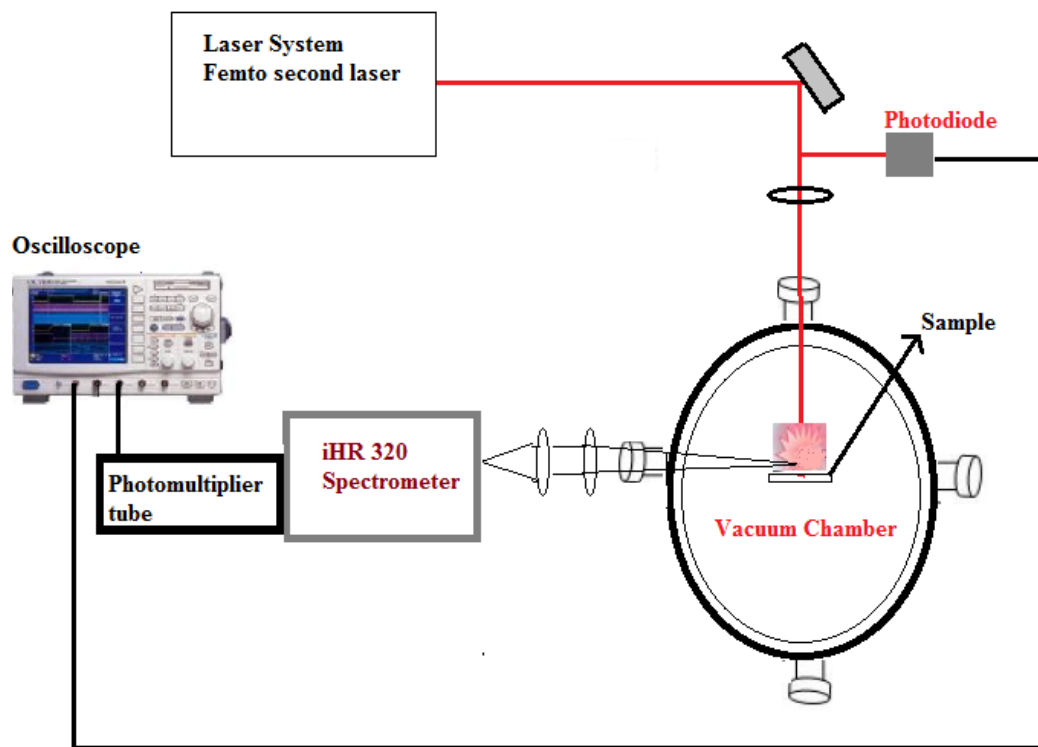


Figure 5.1: Schematic of the experimental set up used for time resolved study laser induced carbon plasma

The plume imaging was accomplished using an intensified CCD camera (4 Picos Stanford Computers) placed orthogonal to the plasma expansion direction. A Nikon lens was used to image the plume region onto the camera to form a two dimensional image of the plume intensity. The visible radiation from the plasma was recorded integrally in the wavelength range 350–900 nm.

5.3 Results and Discussions

In this chapter we have discussed the time resolved spectroscopic study of laser produced copper plasma. Time resolved spectroscopic observations of the femtosecond produced plasma plume from copper under different ambient atmosphere pressure were carried out to determine the life time of the copper lines at various pressure condition.

a) Imaging Results and analysis

Plasma emission begins on the target surface soon after the laser photons reach the surface. Images of the time evolution of the expanding copper plasma were taken at different air pressures ranging from $5\text{E-}6$ torr to 50 torr. Typical ICCD images of the expanding plume at different times after the onset of plasma are given in figures (5.1, 5.2 and 5.3) at different air pressures. These images were recorded at laser irradiance of $890\text{W}/\text{cm}^2$. The duration of the intensification (exposure time) is 10 ns and each image is obtained from a single laser pulse.



Figure5.1: ICCD photographs of visible emission from laser-produced copper plasma at $5\text{e-}6$ Torr background air pressure

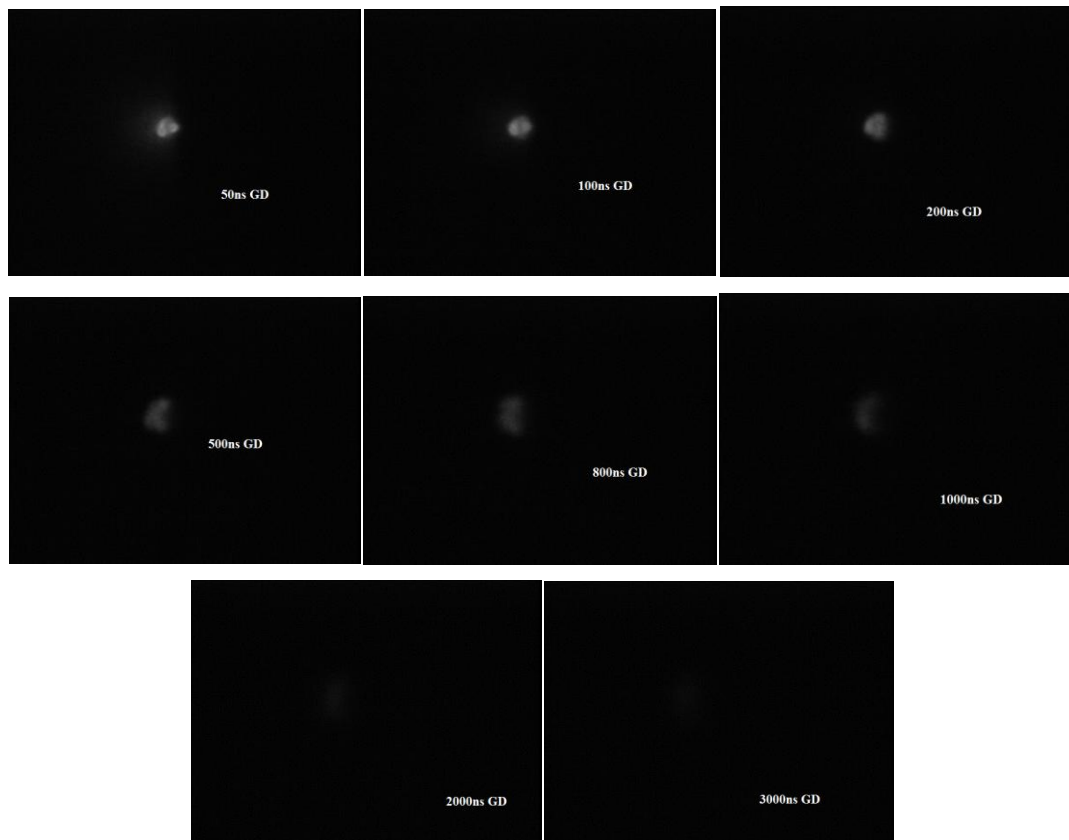


Figure 5.2: ICCD photographs of visible emission from laser-produced copper plasma at 1 Torr background air pressure.

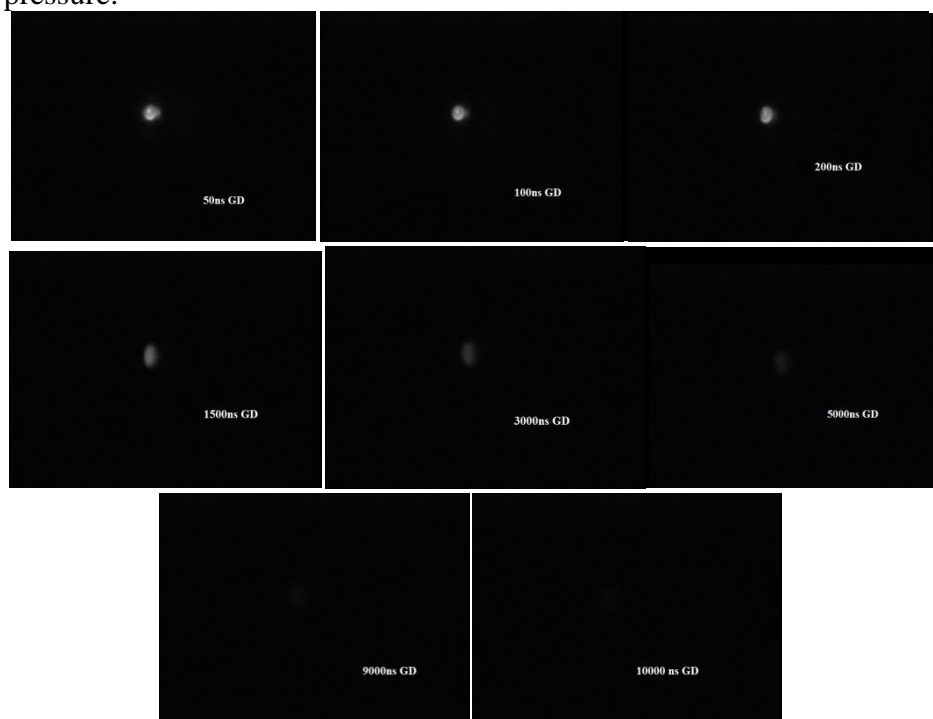


Figure 5.3: ICCD photographs of visible emission from laser-produced copper plasma at 50Torr background air pressure

The Temporal evolution of plasma plume was recorded at different gate delays like 50ns, 100ns, 200ns, 400ns, 500ns, 1000ns, 2000ns etc. At 5E-6 torr air pressure it was observed that plasma expands initially and dyes off at a gate delay of 600ns. And with 1 torr background pressure plasma starts degrading at a gate delay of 500ns and gets completely disappeared at a gate delay of 3000ns. Again increasing the pressure to 50 torr it was observed that initially the plasma expansion is found to be spherical and as time evolves the plasma expands in axial direction and at a gate delay of 10000ns it gets disappeared.

a) Characteristics of lifetimes with pressure change

The dynamics of Cu (I) spectral line 521.820nm at a distance 2mm at different background pressure is as shown in figure 5.4

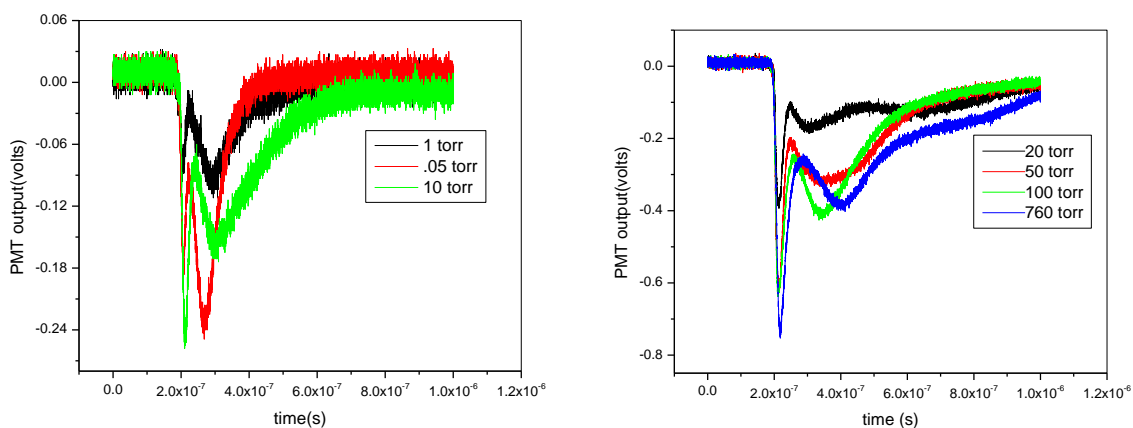


Figure 5.4: The dynamics of Cu (I) spectral line 521.820nm at different pressure

The existence of the double peak were observed in the temporal profile of Cu I 521.820nm (4p ²P -4d ²D) transitions. The double peak i.e., the fast and slow component in the line emission is observed at pressures 5E-2 Torr, 1 Torr, 10 Torr, 20 Torr, 50torr, 100torr and 760torr .Existence of double peak was already reported in the case of metal targets like Aluminum carbon and zinc etc .It is clear that with increasing pressure the first peak becomes more and narrower, while the second one broadens with increase in the ambient pressure. The broadening of the second peak at higher pressure is mainly due to the enhancement in the collisional processes. The faster peak, which arrives with a short time delay, was caused by collisional excitation and ionization atmospheric species by the prompt electrons ejected during the laser target interaction. A delayed and broad component is also observed and that was excited due to bulk plasma electrons. The presence of ambient gas leads to more efficient

electron-impact excitation and plasma recombination, which enhances the emission from these species in the plasma.

Since ultrashort laser pulses can hardly interact with the plasmas they generate, the lifetime of femtosecond laser-induced plasmas is generally shorter than that of nanosecond laser-induced plasmas. The lifetime of the plasma exhibits strong dependence on pressure. The plasma lifetime at different pressures has been determined by measuring the spectral line emission as a function of time. The Elemental lifetimes of neutral atom Cu (I) in different pressure conditions

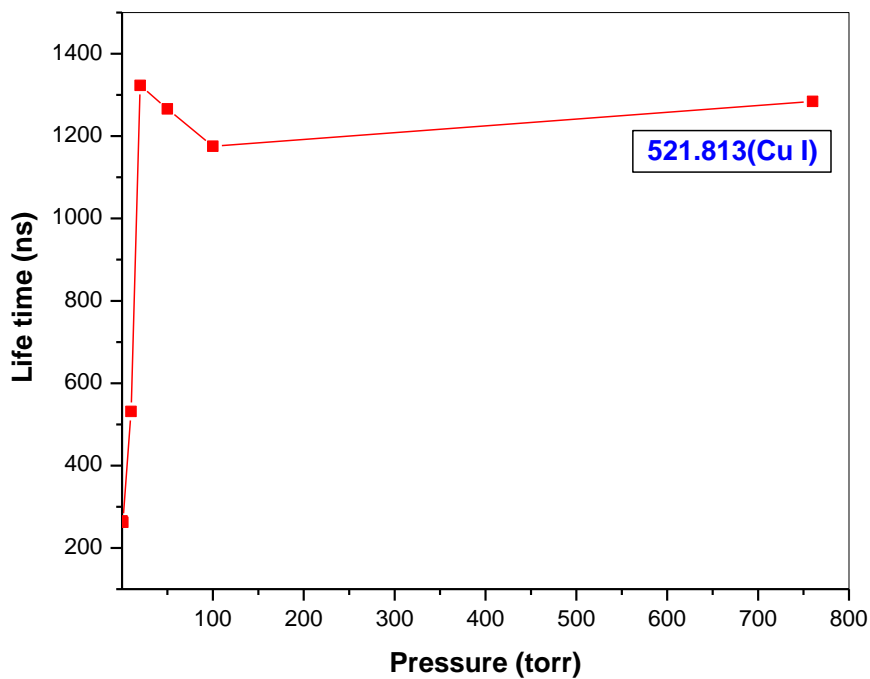


Figure 5.5: Variation of lifetime of Neutral copper line (521.813nm) with ambient pressure

At pressure $10^{-2} < P < 20$ torr

When the pressure is lowered in the medium vacuum range, the elemental lifetime declined for the pressure ranging from 20 to 10^{-2} torr. In general, the effects of plasma cooling and plasma shielding gradually decrease with the decreasing pressure because there is not enough material to take up the heat. Besides, if the mean free path is too large, the small chance of collision makes generation of excitation and ionization difficult. For this reason, there are not enough excited atoms, ions, and electrons for collision with each other, and this causes the elemental lifetime to decrease, despite reducing the plasma cooling effect under this pressure condition.

At pressure $20 < P < 760$ torr

From 760 to 20 torr, most of the elemental lifetimes increase. As mentioned, the low pressure causes reduction in the plasma cooling and shielding effect. During a slow decrease in the plasma temperature, the atoms maintain their excited state for a prolonged period of time. Furthermore the small mean free path around 760 torr results in insufficient collision velocity for generation of strong atomic excitation. At a particular pressure state namely at 20 torr, optimal mean free path for atomic collision is allowed.

The lifetime of Cu I at 20 torr was obtained as 1300ns .The enhancement seen at 20 torr compared to atmosphere (760torr) is likely a result of reduced plasma cooling at low pressures. Plasma cooling occurs when the ambient gas acts as cooling material for the hot vapor plasma. Consequently, the lifetime of LIBS plasma created at 20 torr is much greater than that of a LIBS plasma created at an atmospheric condition.

CHAPTER 6

CONCLUSIONS AND FUTURE OUTLOOK

The interaction of laser radiation with metallic targets is a very useful tool to create plasma plumes consisting of highly concentrated electrons, ions and neutral particles. The presence of a very high pressure gradient makes the plasma evolve in adiabatic expansion into the surrounding vacuum, predominantly along the direction of the target normal.

In this work, a copper target has been irradiated by intense nanosecond and femtosecond laser pulses, and a comparison has been drawn between the resulting plasma spectra. For both nanosecond and femtosecond excitation, the copper LIBS spectra are found to exhibit strong, sharp spectral lines on a significant, continuous background. Plasma parameters like temperature and number density have been calculated for femtosecond and nanosecond produced copper plasma, for different ambient pressure conditions. The emission spectra, electron temperature, and density are found to be significantly influenced by the ambient atmosphere.

The expansion dynamics of copper plasma generated using 800nm ultrafast radiation from a mode-locked Ti: sapphire laser has been investigated using an Intensified CCD (ICCD) camera. Space- and time- resolved emission spectroscopy is done using a monochromator-PMT unit. Temporally resolved emission spectrum of laser induced copper plasma is used to evaluate the space integrated temperature and the electron density as a function of time. Time resolved spectroscopic measurements of femtosecond produced plasma have been carried out to determine the life times of copper lines under different ambient pressures. In the femtosecond regime we have observed the occurrence of slow and fast components in the plasma.

The lifetime of femtosecond laser-induced plasmas is generally shorter than that of nanosecond laser-induced plasmas because ultrashort laser pulses can hardly interact with the plasmas they generate. We found that the plasma lifetime exhibits a strong dependence on ambient pressure. The plasma lifetime at different pressures has been determined by measuring the spectral line emission as a function of time. It is found that the elemental lifetime of neutral copper line (Cu I) increases when the pressure decreases from 760 to 20 torr, and then decreases when the pressure continues to lower down to 10^{-2} torr. The maximum lifetime was observed at 20 torr. This happens due to the plasma cooling and shielding effect, plasma expansion, and the variation in the mean free paths with different surrounding pressures. An analytical study of LIBS with femtosecond laser pulses, under time-resolved

space integrated data acquisition, shows a faster decay of continuum and spectral lines and a shorter plasma lifetime, compared to that excited by longer laser pulses.

An interesting continuation of the work reported in this thesis would be the generation of laser-induced copper plasma in different ambient gases like nitrogen or argon. Similarly, composite materials including nanocomposites may be used as plasma targets, and the constituent elements can be identified. The application of LIBS is extendable to soil analysis and environmental analysis as well.

REFERENCES

1. "Plasma Physics" Richard Fitzpatrick.
2. "Fundamentals of Plasma Physics", James D. Callen, University of Wisconsin, Madison.
3. "Laser-induced breakdown spectroscopy (LIBS) : fundamentals and applications" Andrzej W Miziolek; V Palleschi; Israel Schechter.
4. "Handbook of Laser Induced Breakdown Spectroscopy" by David A. Cremers and Leon J. Radzinski Copyright© 2006 John Wiley & Sons Ltd.
5. "Laser-Induced Breakdown Spectroscopy" By Jagdish P. Sing.
6. Tsunami Mode-locked Ti:sapphire Laser ,User's Manual.
7. Quanta Ray Lab series Pulsed Nd: YAG lasers Users manual.
8. "Breakdown threshold and plasma formation in femtosecond laser–solid interaction" D. von der Linde, H. Schuler .Optical Society of America, 13, 216-222, 1992.
9. "Characteristics of Cu plasma produced by a laser interaction with a solid target" M A Hafez, M A Khedr, F F Elaksher and Y E Gama .Institute of Physics Publishing Plasma Sources Sci. Technol. 12, 185–198, 2003.
10. "Quantitative studies of copper plasma using laser induced breakdown spectroscopy" M. Hanif, M.Salik , M.A.Baig.Optics and Lasers in Engineering 49, 1456–1461, 2011.
11. "Characterization of laser-produced plasma of metal targets "A. Lorusso , L. Velardi, V. Nassisi Radiation Effects & Defects in Solids, 163, 429–433, 2008.
12. "Comparative study of femtosecond and nanosecond laser-induced breakdown spectroscopy of depleted uranium" Luke A. Emmert, Rosemarie C. Chinni, David A. Cremers, C. Randy Jones,and Wolfgang Rudolph. Applied Optics, 50,313-317, 2011 .
13. "Recent Applications of Laser-Induced Breakdown Spectrometry: A Review of Material Approaches" Won-Bae Lee, Jianyong Wu, Yong-Ill Lee,and Joseph Sneddon. Applied Spectroscopic Reviews 39, 27–97, 2004.
14. "Effect of ambient gas conditions on laser-induced copper plasma and surface morphology" Nazar Farid, Shazia Bashir and Khaliq Mahmood Physics Scripta85, 015702, 2012.
15. "Effect of Atmospheric Conditions on LIBS Spectra" Andrew J. Effenberger, Jr. and Jill R. Scott Idaho National Laboratory (INL), 1765 W. Yellowstone HWY, Idaho Falls, ID 83415-2208, USA. Smith, B.W.; Winefordner, J.D.; Omenetto, N. Anal. Bioanal. Chem., 391, 1961-1968. 2008.

16. "Laser-Induced Breakdown Spectroscopy: Capabilities and Applications" Jennifer L. Gottfried and Frank C. De Lucia, Jr.
17. "Laser-Induced Plasma Formation in Water at Nanosecond to Femtosecond Time Scales: Calculation of Thresholds, Absorption Coefficients, and Energy Density" Joachim Noack and Alfred Voge IEEE Journal of Quantum Electronics, 35, 1156-1167, 1999.
18. "Measurements of plasma temperature and electron density in laser-induced copper plasma by time-resolved spectroscopy of neutral atom and ion emissions" V K Unnikrishnan, Kamlesh Alti, V B Kartha, C Santhosh, G P Gupta and B M Suri .Pramana J. Phys, 74, 983-993, 2010.
19. "Laser-induced plasma peculiarity at low pressures from the elemental lifetime perspective" Soo-Jin Choi and Jack J. Yoh .Optics Express 19, No. 23 / 23098 2011.
20. "Characterization of laser – induced plasmas by atomic emission spectroscopy" Diego M Díaz Pace, Graciela Bertuccelli, and Cristian A D'Angelo, Journal of Physics: Conference Series 274, 012076, 2011.
21. "Temporal and spatial evolution of laser ablated plasma from $\text{YBa}_2\text{Cu}_3\text{O}_7$ " S. S. Harilal, P. Radhakrishnan, V. P. N. Nampoori, and C. P. G. Vallabhan. Appl. Phys. Lett. 64 (25), 3377-3379, 1994.
22. "Pressure dependence of emission intensity in femtosecond laser-induced breakdown spectroscopy" Serife Yalc, m, Ying Y. Tsui and Robert Fedosejevs. J. Anal. At. Spectrom , 19 , 1295 – 1301, 2004.
23. "Measurement of electron density and temperature of a laser-induced zinc plasma", Nek M Shaikhet al. J. Phys. D: Appl. Phys. 39 1384. 2006.
24. "Laser Induced Plasma Spectroscopy (LIPS) as an efficient method for elemental analysis of environmental samples" ,M. Kompitsas, F. Roubani-Kalantzopoulou, Bassiotis A. Diamantopoulou and A. Giannoudakos , Proceedings of EARSeL-SIG-Workshop LIDAR, Dresden/FRG, June 16 – 17, 2000

